認め，9例が7歳から36歳に除鉄療法を開始されている．解析時には5例の死亡例で死亡年齢は31～57歳，心疾患，肝疾患が3例，耳の扁平上皮癌が1例，敗血症が1例であった．

日本における十分な調査はなされていないが，小児例に対する多賀らの2006年の全国調査では，12例中5例が死亡，1例が輸血依存，1例が同種造血幹細胞移植，1例が摘脾，3例が無治療で生存中であった[12]．

日本における現状と今後の課題

わが国においては，2006年の多賀らの全国調査では，少数ながらCDA患者が存在することが確認された[12]．しかしながら，この調査が日本小児血液学会再生不良性貧血委員会の調査であり，実態が十分把握できていない可能性があると思われ，本疾患に遭遇する機会が多いであろう新生児医療に携わる医師を含む小児科学会員や成人例を担当する血液内科医を含む日本血液学会員への調査を厚生労働省班研究（真部班）が中心に行い，本疾患への関心が高まり，診断の相談や問合せ，遺伝子検査の依頼（現在名古屋大学小児科で*CDA1*, *SBC23B*などの検査を実施中）が増えている[13]．すでに遺伝子変異が見つかっている症例もある（Doisaki S, unpublished data）．今度もさらなる本疾患の啓蒙を行いつつ，中央診断や遺伝子検査を取り入れることで我が国におけるCDAの的確な診断と症例の把握が行われることを期待したい．

文　献

1) Heimple H, Wendt F. Congenital dyserythropoietic anemia with karyorrhexis and multinuclearity of erythroblasts. Helv Med Acta 1968；34：103—115.
2) Tamary H, Shalv H, Liria D, et al. Clinical features and studies of erythropoiesis in Israeli Bedouins with congenital dyserythropoietic anemia type I. Blood 1996；87：1763—1770.
3) Tamary H, Shalev H, Perez-Avraham G, et al. Elevated growth differention factor 15 expression in patients with congenital dyserythropoietic anemia type I. Blood 2008；112：5241—5244.
4) Dgany O, Avidan N, Delaunay J, et al. Congenital dyserythropoietic anemia type I ins caused by mutations in codanin-1. American J Hum Genet 2002；71：1467—1474.
5) Noy-Lotan S, Dgany O, Lahmi R, et al. Codanin-1, the protein encode by the gene mutated in CDA-1 (CDAN1), is cell cycle regulated. 50th Annual Meeting of the American Society of Hematology. San Francisco, USA, 2008.
6) Iolascon A, D'Aostaro G, Perrotta S, et al. Congenital dyserythropoietic anemia type II：molecular basis and clinical aspects. Haematologica 1996；81：543—559.
7) Schwarz K, Iolascon A, Verissimo F, et al. Mutations affecting the secretory COPII coat component SEC23B cause congenital dyserythropoietic anemia type II. Nat Genet 2009；41：936—940.
8) Iolascon A, Russo R, Delaunay J. Congenital dyserythropoietic anemias. Current Opinion in Hematology 2011；18：146—151.
9) Heimpel H. Congenital dyserythropoietic anemias：epidemiology, clinical significance, and progress in understanding their pathogenesis. Ann Hematol 2004；83：613—621.
10) Wickramasinghe SN, Wood WG. Advances in the understanding of the congenital dyserythropoietic anaemias. Bri J Haematol 2005；131：431—446.
11) Heimpel H, Schwarz K, Ebnöther M, et al. Congenital dyserythropoietic anemia type I (CDA I)：molecular genetics, clinical appearance, and prognosis based on long-term observation. Blood 2006；107：334—340.
12) 多賀　崇，伊藤　剛，浅見恵子，他．Congenital dyserythropoietic anemiaの全国調査．日小血誌 2008；22：233—238.
13) Kamiya T, Manabe A. Congenital dyserythropoietic anemia. Int J Hematol 2010；92：432—438.

INTERNAL MEDICINE

□ CASE REPORT □

A Case of Congenital Dyserythropoietic Anemia Type 1 in a Japanese Adult with a *CDAN1* Gene Mutation and an Inappropriately Low Serum Hepcidin-25 Level

Hiroshi Kawabata[1], Sayoko Doisaki[2], Akio Okamoto[3], Tatsuki Uchiyama[1], Soichiro Sakamoto[1], Asahito Hama[2], Kiminori Hosoda[4], Junji Fujikura[5], Hitoshi Kanno[6], Hisaichi Fujii[6], Naohisa Tomosugi[7], Kazuwa Nakao[5], Seiji Kojima[2] and Akifumi Takaori-Kondo[1]

Abstract

We describe the first case of genetically diagnosed congenital dyserythropoietic anemia (CDA) type 1 in a Japanese man. The patient had hemolytic anemia since he was a child, and he developed diabetes, hypogonadism, and liver dysfunction in his thirties, presumably from systemic iron overload. When he was 48 years old a diagnosis was finally made by genetic analysis that revealed a homozygous mutation of *CDAN1* gene (Pro1129Leu). His serum hepcidin-25 level was inappropriately low. We conclude that physicians should be aware of the possibility of CDA in a patient with anemia and systemic iron overload at any age.

Key words: congenital dyserythropoietic anemia, iron metabolism, hemochromatosis, hepcidin, growth differentiation factor-15

(Intern Med 51: 917-920, 2012)
(DOI: 10.2169/internalmedicine.51.6978)

Introduction

Congenital dyserythropoietic anemia (CDA) is a rare congenital erythropoietic disorder with characteristic morphological abnormalities of the bone marrow cells, ineffective erythropoiesis and systemic iron overload (1). Three types of CDA are known: types 1, 2 and 3. The genes responsible for types 1 and 2 have recently been identified as *CDAN1* and *SEC23B*, respectively (2, 3). Both CDA types 1 and 2 are inherited recessively. The incidence of CDA is very rare, and in a recent pan-European survey, only 124 CDA type 1 cases were recorded (4). To date, several Japanese CDA type 1 cases have also been reported (5-7), but none of them has been genetically proven. Here, we describe in a Japanese adult a case of CDA type 1 with systemic iron overload that was genetically diagnosed in his late forties.

Case Report

A Japanese man was referred to the Kyoto University Hospital for hyperglycemia when he was 38 years old. He had had hemolytic anemia since he was a child, but its etiology had not been determined. He had undergone splenectomy when he was 36 years old, which ameliorated his anemia to some extent. At his first visit to our hospital, his white blood cell count was 6,400/μL; red blood cell count, 1.93×10^6/μL; hemoglobin (Hb) level, 7.5 g/dL; hematocrit level, 21.0%; mean corpuscular volume, 108.8 fL; platelet count, 365×10^3/μL; and reticulocyte count, 53×10^3/μL (Ta-

[1]Department of Hematology and Oncology, Graduate School of Medicine, Kyoto University, Japan, [2]Department of Pediatrics, Nagoya University Graduate School of Medicine, Japan, [3]Nantan General Hospital, Japan, [4]Faculty of Human Health Science, Kyoto University Graduate School of Medicine, Japan, [5]Department of Medicine and Clinical Science, Kyoto University Graduate School of Medicine, Japan, [6]Department of Transfusion Medicine and Cell Processing, Tokyo Women's Medical University, Japan and [7]Division of Advanced Medicine, Medical Research Institute, Kanazawa Medical University, Japan
Received for publication November 21, 2011; Accepted for publication January 5, 2012
Correspondence to Dr. Hiroshi Kawabata, hkawabat@kuhp.kyoto-u.ac.jp

Table 1. **Laboratory Data**

Features	Laboratory data at the first visit (38 years old)	Laboratory data at the time of diagnosis (48 years old)
White blood cells (per μL)	6.4×10^3	5.3×10^3
Red blood cells (per μL)	1.93×10^6	2.41×10^6
Hemoglobin (g/dL)	7.5	8.5
Hematocrit (%)	21.0	24.1
Reticulocytes (per μL)	53×10^3	—
Platelet counts (per μL)	365×10^3	312×10^3
Total bilirubin (mg/dL)	1.5	1.6
Direct bilirubin (mg/dL)	0.7	0.1
Haptoglobin (mg/dL)	<7.9	—
AST (IU/L)	49	26
ALT (IU/L)	68	16
LDH (IU/L)	302	277
Ferritin (ng/mL)	4058	186

— indicates that the tests were not performed. Abbreviations; AST, aspartate aminotransferase (reference range, 13-29 IU/L); ALT, alanine aminotransferase (reference range, 8-28 IU/L); LDH, lactate dehydrogenase (reference range, 129-241 IU/L).

ble 1). He had hepatic dysfunction, with a slightly elevated serum alanine aminotransferase level (68 IU/L), hyperglycemia (blood sugar level of 146 mg/dL and HbA1c level of 6.9%) with very low insulin secretion (serum c-peptide level, <0.1 ng/mL), and hypogonadism with a serum testosterone level lower than 0.2 ng/mL, i.e., very low (reference range, 2.7-10.7 ng/mL). His blood test results also suggested iron overload (transferrin saturation of 95.3% and serum ferritin level of 4,058 ng/mL), and the liver biopsy results revealed marked accumulation of iron in the parenchymal cells. Thus, hemochromatosis, along with liver dysfunction, diabetes and hypogonadism, was diagnosed. Insulin therapy was then started. Occasional phlebotomy was also started to remove excess iron and to gradually decrease his serum ferritin and alanine aminotransferase levels to within the reference ranges (Table 1). When he was 46 years old, a series of intensive diagnostic examinations were started. The findings of the biochemical analyses for erythrocyte membrane disorders or unstable hemoglobinopathies were all negative. The bone marrow examination revealed marked erythroid hyperplasia (the myeloid to erythroid ratio of 0.34) and remarkable dysplastic features in the erythroid cells, with megaloblastoid changes and multinuclear cells (Fig. 1A-E). However, no significant dysplasia was observed in the granulocytic or megakaryocytic series (Fig. 1A, B), and no ring sideroblasts were observed in the iron staining. When he was 48 years old, we obtained his written informed consent and approval by the ethics committee of Kyoto University to perform a genetic analysis for indicators of hereditary iron disorders in his peripheral blood cells. The results of the genetic analyses for pyruvate kinase deficiency and thalassemia syndromes were all negative. There were no mutations in the exons and the exon-intron borders of hereditary hemochromatosis genes including *HFE*, *TFR2*, *HJV*, *HAMP*, and *SLC40A1*. However, a homozygous mutation in *CDAN1 ex26 c.3503 C>T* (Pro1129Leu) was detected, consistent with CDA type 1 (Fig. 2). When we reviewed his bone marrow specimen, internuclear bridges that connected two separate erythroblasts were occasionally observed (7 bridges in 500 erythroblasts, Fig. 1F-J). His serum hepcidin-25 level was 0.8 ng/mL [reference range, 2.3-37 ng/mL; analyzed with a quantitative liquid chromatography coupled with tandem mass spectrometry method (8)]. The growth differentiation factor-15 (GDF15) level was 8,469 pg/mL (reference range, 215-835 pg/mL; analyzed with a commercial ELISA kit from R&D, Minneapolis, MN). The patient had two siblings, a brother and a sister; both were in good health. There was no significant family history except that his mother had anemia of undetermined etiology, and his paternal grandfather had diabetes. He declined genetic analysis of his family for the *CDAN1* gene.

Discussion

We encountered an adult patient with hemolytic anemia with various symptoms caused by systemic iron overload, who turned out to have a genetic mutation consistent with CDA type 1. To our knowledge, this is the first documented case of CDA type 1 in a Japanese with *CDAN1* gene mutation. Dgany et al. identified the same *CDAN1* gene mutation as the current case in a French Polynesian family (2). *CDAN1* is located on chromosome 15q15.1-15q15.3, and it codes for a nuclear protein, codanin-1, the human homolog of discs lost (dlt) which is required for cell survival and cell cycle progression in *Drosophila* (9). The diagnosis of CDA type 1 has usually been made from clinical features together with characteristic morphological features of the bone marrow cells such as binucleated erythroblasts, and internuclear bridges between the erythroid cells. As codanin-1 is essential for proper cellular trafficking of the heterochromatin

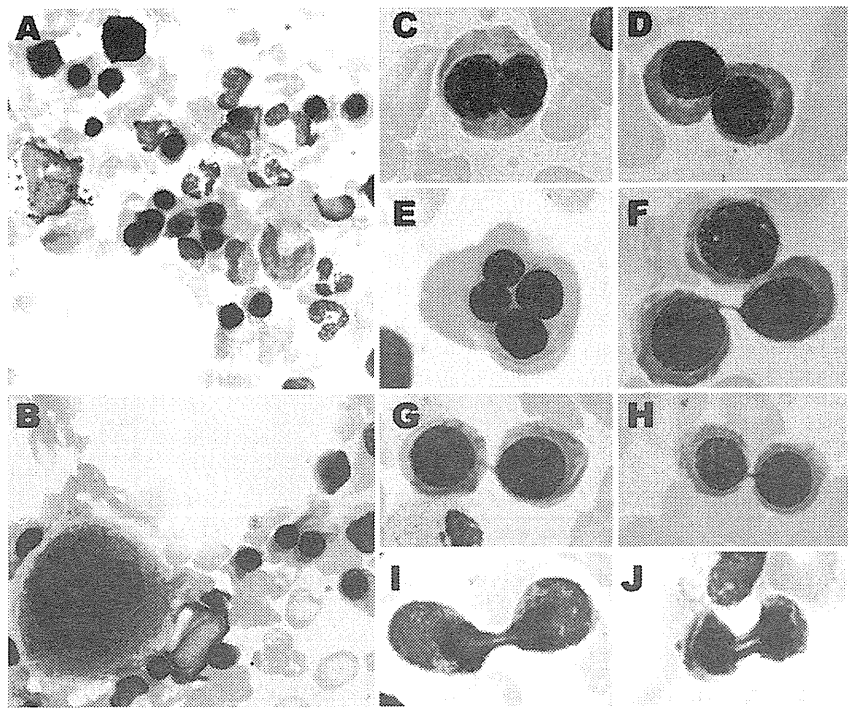

Figure 1. **Bone marrow cell morphology (May-Grünwald-Giemsa staining, original magnification ×1,000; C-J, images were further magnified by photographic enlargement). A and B: Erythroid hyperplasia. No significant dysplasia was observed in the granulocytic or megakaryocytic series. C and D: Binucleated erythroblasts. These cells were found in approximately 12% of the erythroblasts. E: A few tetranucleated erythroblasts were found. F-J: Internuclear bridges between the erythroblasts were found after careful inspection.**

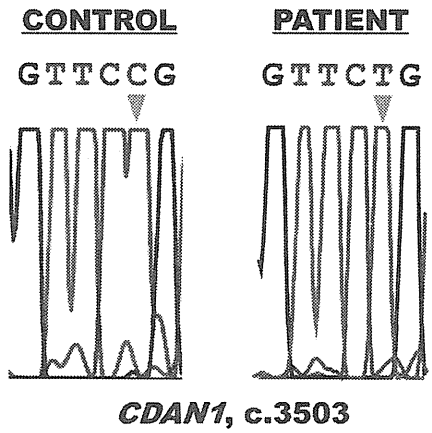

Figure 2. **The homozygous mutation in *CDAN1* (*ex26 c.3503 C>T*, Pro1129Leu) detected in the patient.**

protein HP1-α (10), defects of this protein may result in such morphological abnormalities. In the current case, the bone marrow examination results showed numerous binucleated erythroblasts, but the internuclear bridges, which are much more specific features of this disorder, were observed in less than 3% of the erythroblasts and were overlooked in the first inspection (Fig. 1). Therefore, making a definitive diagnosis of CDA from bone marrow cell morphology alone can sometimes be difficult.

CDA types 1 and 2 are known to be accompanied by iron overload. Similar to hereditary hemochromatosis, inappropriately low production of hepcidin, the central regulator of systemic iron homeostasis, has been proposed as the etiology of iron overload in CDA (11). As the main function of hepcidin is to downregulate the expression of ferroportin, the only known cellular iron exporter of mammals, downregulation of hepcidin results in an increase in ferroportin expression, thereby increasing iron absorption from the intestine and causing systemic iron overload. A previous report demonstrated marked increases of GDF15 in the serum of CDA type 1 patients (12). GDF15, a humoral factor belonging to the transforming growth factor-β superfamily, has been shown to suppress hepatic production of hepcidin (13). Consistent with the previous reports, systemic iron overload was induced in the current case without repeated red cell transfusions, the serum GDF15 level was remarkably elevated, and the serum hepcidin-25 level was inappropriately low. Thus, we postulate that serum hepcidin-25 and GDF15 are useful markers for CDA.

CDA is generally regarded as a pediatric disease because the initial symptoms, such as anemia, jaundice, and splenomegaly, usually appear in the first decade. However, the current case was diagnosed when the patient was in his late forties, and in the pan-European survey, CDA was diag-

nosed in a substantial proportion of patients who were middle-aged or older (4). Early diagnosis of CDA is important because iron chelation therapy (or phlebotomy if anemia is mild) should be started as early as possible to avoid iron overload, which can cause irreversible tissue damage. In addition, interferon-α is known to be effective for ameliorating anemia and iron accumulation in patients with CDA type 1, although the precise mechanism is still unknown (14). The survey data and our findings of the current case suggest that we should be aware of the possibility of CDA in patients with anemia and systemic iron overload at any age.

The authors state that they have no Conflict of Interest (COI).

References

1. Kamiya T, Manabe A. Congenital dyserythropoietic anemia. Int J Hematol **92**: 432-438, 2010.
2. Dgany O, Avidan N, Delaunay J, et al. Congenital dyserythropoietic anemia type I is caused by mutations in codanin-1. Am J Hum Genet **71**: 1467-1474, 2002.
3. Schwarz K, Iolascon A, Verissimo F, et al. Mutations affecting the secretory COPII coat component SEC23B cause congenital dyserythropoietic anemia type II. Nat Genet **41**: 936-940, 2009.
4. Heimpel H, Matuschek A, Ahmed M, et al. Frequency of congenital dyserythropoietic anemias in Europe. Eur J Haematol **85**: 20-25, 2010.
5. Kuribayashi T, Uchida S, Kuroume T, Umegae S, Omine M, Maekawa T. Congenital dyserythropoietic anemia type I: report of a pair of siblings in Japan. Blut **39**: 201-209, 1979.
6. Hiraoka A, Kanayama Y, Yonezawa T, Kitani T, Tarui S, Hashimoto PH. Congenital dyserythropoietic anemia type I: a freeze-fracture and thin section electron microscopic study. Blut **46**: 329-338, 1983.
7. Kato K, Sugitani M, Kawataki M, et al. Congenital dyserythropoietic anemia type 1 with fetal onset of severe anemia. J Pediatr Hematol Oncol **23**: 63-66, 2001.
8. Kanda J, Mizumoto C, Kawabata H, et al. Serum hepcidin level and erythropoietic activity after hematopoietic stem cell transplantation. Haematologica **93**: 1550-1554, 2008.
9. Pielage J, Stork T, Bunse I, Klämbt C. The Drosophila cell survival gene discs lost encodes a cytoplasmic Codanin-1-like protein, not a homolog of tight junction PDZ protein Patj. Dev Cell **5**: 841-851, 2003.
10. Renella R, Roberts NA, Brown JM, et al. Codanin-1 mutations in congenital dyserythropoietic anemia type 1 affect HP1α localization in erythroblasts. Blood **117**: 6928-6938, 2011.
11. Ganz T. Hepcidin and iron regulation, 10 years later. Blood **117**: 4425-4433, 2011.
12. Tamary H, Shalev H, Perez-Avraham G, et al. Elevated growth differentiation factor 15 expression in patients with congenital dyserythropoietic anemia type I. Blood **112**: 5241-5244, 2008.
13. Tanno T, Bhanu NV, Oneal PA, et al. High levels of GDF15 in thalassemia suppress expression of the iron regulatory protein hepcidin. Nat Med **13**: 1096-1101, 2007.
14. Lavabre-Bertrand T, Blanc P, Navarro R, et al. alpha-Interferon therapy for congenital dyserythropoiesis type I. Br J Haematol **89**: 929-932, 1995.

Int J Hematol (2012) 95:675–679
DOI 10.1007/s12185-012-1079-9

ORIGINAL ARTICLE

Excellent outcome of allogeneic bone marrow transplantation for Fanconi anemia using fludarabine-based reduced-intensity conditioning regimen

Akira Shimada · Yoshiyuki Takahashi · Hideki Muramatsu · Asahito Hama · Olfat Ismael · Atsushi Narita · Hiroshi Sakaguchi · Sayoko Doisaki · Nobuhiro Nishio · Makito Tanaka · Nao Yoshida · Kimikazu Matsumoto · Koji Kato · Nobuhiro Watanabe · Seiji Kojima

Received: 21 October 2011 / Revised: 5 April 2012 / Accepted: 5 April 2012 / Published online: 22 April 2012

Abstract Fanconi anemia (FA) is a disorder characterized by developmental anomalies, bone marrow failure and a predisposition to malignancy. It has recently been shown that hematopoietic stem cell transplantation using fludarabine (FLU)-based reduced-intensity conditioning is an efficient and quite safe therapeutic modality. We retrospectively analyzed the outcome of bone marrow transplantation (BMT) in eight patients with FA performed in two institutes between 2001 and 2011. There were seven females and one male with a median age at diagnosis = 4.5 years (range 2–12 years). The constitutional characteristics associated with FA, such as developmental anomalies, short stature and skin pigmentation, were absent in three of the patients. One patient showed myelodysplastic features at the time of BMT. All patients received BMT using FLU, cyclophosphamide (CY) and rabbit antithymocyte globulin (ATG) either from a related donor ($n = 4$) or an unrelated donor ($n = 4$). Acute graft-versus-host disease (GVHD) of grade I developed in one patient, while chronic GVHD was not observed in any patient. All patients are alive and achieved hematopoietic recovery at a median follow-up of 72 months (range 4–117 months). BMT using FLU/low-dose CY/ATG -based regimens regardless to the donor is a beneficial therapeutic approach for FA patients.

Keywords Fanconi anemia · Hematopoietic stem cell transplantation · Fludarabine

A. Shimada · Y. Takahashi · H. Muramatsu · A. Hama · O. Ismael · A. Narita · H. Sakaguchi · S. Doisaki · N. Nishio · M. Tanaka · S. Kojima (✉)
Department of Pediatrics,
Nagoya University Graduate School of Medicine,
65 Tsurumai-cho, Showa-ku, Nagoya, Aichi 466-8550, Japan
e-mail: kojimas@med.nagoya-u.ac.jp

A. Shimada
e-mail: ashimada@med.nagoya-u.ac.jp

N. Yoshida · K. Matsumoto · K. Kato
Department of Pediatric Hematology/Oncology,
Nagoya First Red Cross Hospital, 3-35 Dougecho,
Nakamuraku, Nagoya 453-8511, Japan

N. Watanabe
Department of Pediatrics, Cyukyo Hospital,
1-1-10 Sanjo, Minamiku, Nagoya 457-0866, Japan

Introduction

Fanconi anemia (FA) is a complex disorder characterized by developmental anomalies, early onset progressive bone marrow failure (BMF) and a tendency to develop hematological and non-hematological malignancies. The risk of FA patients to develop BMF and malignancies increases with progression of age, and the cumulative incidence by age of 40 years was 90 % for BMF and 30 % for hematologic and nonhematologic neoplasms [1–4]. Short stature and abnormal skin pigmentation are particularly common features found in patients with FA and a wide variety of congenital malformations has been described in 60–75 % of FA patients [3–5]. The incidence of FA in Japan was approximately 5–10 new cases diagnosed annually and hematological abnormalities usually manifested early in childhood at a median age of 7 years (range 0–31 years). Owing to the complexity of the disease and multisystem involvement, FA has a high mortality rate with a median age of death of 30 years [3–5]. Therefore, the study of FA holds a great promise for elucidation of the heterogeneity of this disorder in the future. Hematopoietic stem cell transplantation (HSCT) is the only curative therapy known so far for correcting the hematological manifestations in

Table 1 Clinical characteristics of 8 Fanconi anemia patients

No.	Male/ female	Disease status at HSCT	Age at diagnosis (year)	Age at HSCT (year)	Karyotype	Chromosomal fragility test (gap and break/100 cells)	Short stature (<−1SD)	Skin pigmentation	Other anomalies
1	F	SAA	7	8	46,XX	114	No	No	No
2	F	SAA	3	5	46,XX	514	−2SD	Yes	Shortness of first finger
3	F	SAA	8	8	46,XX	193	No	No	No
4	F	SAA	12	13	46,XX	299	−1SD	Yes	No
5	M	SAA	2	7	46,XY	152	−3SD	No	Hyperdactylia
6	F	MDS (RAEB)	3	6	Other[a]	148	−1.5SD	No	Hyperdactylia
7	F	SAA	6	11	46,XX	159	No	No	No
8	F	SAA	3	5	46,XX	169	−2SD	Yes	Radius defect, esophageal atresia

SAA severe aplastic anemia, *MDS* myelodysplastic syndrome, *HSCT* hematopoietic stem cell transplantation, *RAEB* refractory anemia with excess blasts

[a] others; 46,XX,add(3)(q26),der(7)add(7)(p22)add(7)(q11)add(8)(q22)

FA patients. Initially, potential problems in designing HSCT conditioning regimens for patients with FA appeared due to the acquired hypersensitivity to DNA cross-linking or oxidative agents such as alkylating agents or ionizing radiation [6], but recently a significant progress has been achieved by using FLU-based reduced-intensity conditioning regimens that markedly improved the efficiency and safety of this procedure [7, 8]. Specifically, FLU-based reduced-intensity conditioning allogeneic HSCT resulted in reduction of regimen-related toxicity (RRT), superior engraftment and less graft-versus-host disease (GVHD), which in turn led to improvement of patients' survival. In this study, we aimed to investigate the effectiveness and safety profile of bone marrow transplantation (BMT) using FLU-based reduced-intensity conditioning regimens in eight patients with FA, who were transplanted from either a related donor (3 HLA-genetically matched and 1 HLA-A locus mismatched) or an unrelated donor (2 HLA-matched and 2 HLA-DRB1 mismatched).

Patients and methods

We retrospectively analyzed eight patients, who were diagnosed as having FA and received BMT at Nagoya University and Nagoya First Red Cross Hospital between 2001 and 2011. There were seven females and one male with a median age at diagnosis of 4.5 years (range 2–12 years) (Table 1). Clinical features suggestive of FA including low birth weight, short stature, hyperpigmented skin, radial abnormality and duplicated thumbs were defined in five out of eight patients, while three patients were asymptomatic. Diagnosis of FA was confirmed in all patients by a reliable cellular marker for FA cells and all of them showed a high incidence of chromosomal breaks and gaps, which indicated chromosomal instability by adding mitomycin C at a final concentration of 0.5 μM (Table 1). Seven patients suffered from severe aplastic anemia and one patient evolved to refractory anemia with excess of blasts (RAEB) with the emergence of cytogenetic abnormalities in the form of add(3)(q26) at the time of HSCT. All patients underwent allogeneic BMT at a median age of 7.5 years (range 5–13 years), and they were transplanted from either a related donor (3 HLA-genetically matched and 1 HLA-A locus mismatched) or an unrelated donor (2 HLA- matched and 2 HLA-DRB1 mismatched). All patients received a preparative regimen including a combination of fludarabine (FLU 120–180 mg/m^2), cyclophosphamide (CY 40 mg/kg) and rabbit anti-thymocyte globulin (ATG, Thymoglobulin, Genzyme, 5–10 mg/kg). Patients transplanted from unrelated donor received a total body irradiation (TBI)/total lymphoid irradiation (TLI) of 4–4.5 Gy, and patients transplanted from HLA-A locus mismatched related donor received 2 Gy. As GVHD prophylaxis, BM recipients from related donor received cyclosporine A (CyA) plus short-term methotrexate (MTX), while BM recipients from unrelated donor received tacrolimus (FK506) plus short-term MTX. Details on the donors' characteristics, conditioning regimen and GVHD prophylaxis are listed in Table 2.

Table 2 Hematopoietic stem cell transplantation for 8 Fanconi anemia patients

No.	Performance status	Transfusion before SCT	Conditioning	Donor	Concordance of HLA-serological typing	Transfused cell number ($\times 10^8$/kg)	GVHD prophylaxis
1	0	MAP 2u, PC10u	FLU (120 mg/m^2) + CY (40 mg/kg) + ATG (10 mg/kg)	Mother	6/6	3.9	CyA + short MTX
2	0	MAP 2u, PC10u	FLU (150 mg/m^2) + CY (40 mg/kg) + ATG (6 mg/kg)	Sister	6/6	7.4	CyA + short MTX
3	0	MAP 4u, PC 20u	FLU (180 mg/m^2) + CY (40 mg/kg) + ATG (10 mg/kg) + TBI (2 Gy)	Father	5/6 (mismatched A 1 locus)	3.0	CyA + short MTX
4	0	MAP 4u, PC 20u	FLU (150 mg/m^2) + CY (40 mg/kg) + ATG (5 mg/kg)	Brother	6/6	2.2	CyA + short MTX
5	1	MAP 21u, PC 120u	FLU(180 mg/m^2) + CY(40 mg/kg) + ATG(10 mg/kg) + TLI (4 Gy)	Unrelated	6/6	3.0	FK506 + short MTX
6	0	MAP 16u, PC100u	FLU (150 mg/m^2) + CY (40 mg/kg) + ATG (10 mg/kg) + TBI (4.5 Gy)	Unrelated	5/6 (mismatched DR 1 locus)	4.5	FK506 + short MTX
7	0	MAP 12u, PC120u	FLU (120 mg/m^2) + CY (40 mg/kg) + ATG (10 mg/kg) + TLI (4 Gy)	Unrelated	5/6 (mismatched DR 1 locus)	3.8	FK506 + short MTX
8	0	MAP 4u, PC 20u	FLU (150 mg/m^2) + CY (40 mg/kg) + ATG (10 mg/kg) + TBI (4.5 Gy)	Unrelated	6/6	4.6	FK506 + short MTX

SCT stem cell transplantation, *FLU* fludarabine, *CY* cyclophosphamide, *ATG* anti-thymocyte globulin (rabbit ATG, Thymoglobulin), *TBI* total body irradiation, *TLI* total lymphoid irradiation, *CyA + short MTX* cyclosporine plus short-term methotrexate

Results

The median transfused nucleated cell number was 3.8 × 10^8/kg (range 2.2 to 7.4 × 10^8/kg) and all patients achieved sustained engraftment; the median time to neutrophil (>500), platelet (>50,000/ml) and reticulocyte (>10‰) recovery was 15.5, 20.5 and 21.5 days, respectively. Among eight patients enrolled in this study with a median survival period of 72 months (range 4–117 months), acute GVHD grade I was detected in one patient, whereas chronic GVHD was not found in any patient. Two patients experienced hepatic dysfunction and one patient had gastric hemorrhage as regimen-related toxicities (grade 1 according to the National Cancer Institution-Common Toxicity Criteria, NCI-CTC Version 4.0). Three patients exhibited febrile neutropenia and one of them showed disseminated fungal infection (grade 4 according to NCI-CTC) complicated by development of a renal abscess that showed complete remission after amphotericin B treatment. Cytomegalovirus (CMV)-polymerase chain reaction (PCR) and CMV-pp65 antigen detection were performed on a weekly basis for identification of CMV infection. We found four out of eight patients showed CMV reactivation without clinical symptom and they were treated with ganciclovir and foscavir. One patient suffered from hemorrhagic cystitis and lymphoproliferative disorder (LPD) due to BK virus and Epstein–Barr virus (EBV) reactivation, respectively. This patient was completely cured from the EBV–LPD after successful treatment with rituximab. Otherwise, no patients developed veno-occlusive disease (VOD) or thrombotic microangiopathy (TMA) (Table 3). Over the total length of the follow-up period, no patients showed secondary bone marrow failure and/or malignancies with a median follow-up of 72 months (range 4–117 months).

Discussion

Through a retrospective analysis of the medical records of eight pediatric patients with FA, who received FLU-based reduced-intensity conditioning allogeneic HSCT to evaluate their outcome, we found that all patients achieved favorable outcome using this procedure and the type of the donor did not significantly influence the clinical outcome. In previous studies, it has been proved that the use of alkylating agents and radiation therapy for FA patients was harmful. The impact of lower irradiation dose on immune recovery and risk of malignancy remains a matter of debate and a longer follow-up period is needed. However, it was reported that TBI 300 cGy was the lowest possible irradiation dose in the context of FLU/CY-based regimen; other

Table 3 Results of hematopoietic stem cell transplantation for 8 Fanconi anemia patients

No.	Days of engraftment	Acute GVHD	Chronic GVHD	RRT	VOD	TMA	CMV Ag positivity and treatment	Other virus related disease	FN	Fungal infection	Overall survival (Mo)
1	19	0	0	No	No	No	Day 35, GCV	No	No	No	114
2	15	I	0	No	No	No	Day 13, GCV + FCV	No	Yes	No	41
3	19	0	0	Liver dysfunction (grade 1)	No	No	Day 30, GCV	No	Yes	No	17
4	14	0	0	Gastric hemorrhage (grade 1)	No	No	No	No	No	No	4
5	17	0	0	No	No	No	Day 48, GCV	No	No	No	117
6	19	0	0	No	No	No	No	No	No	Disseminated fungal infection, renal abscess (grade 4)	99
7	15	0	0	Diarrhea (grade 1), liver dysfunction (grade 1)	No	No	No	Hemorrhagic cystitis due to BKV (grade 2) and LPD due to EBV	Yes	No	72
8	19	0	0	No	No	No	No	No	No	No	26

RRT grade was determined by National Cancer Institute-Common Toxicity Criteria (NCI-CTC Ver 4.0)

GVHD graft-versus-host disease, *RRT* regimen-related toxicity, *VOD* veno-occlusive disease, *TMA* thrombotic microangiopathy, *CMV Ag* AMV antigenemia (pp65), *GCV* ganciclovir, *FCV* foscavir, *BKV* BK virus, *EBV*, Epstein–Barr virus, *FN* febrile neutropenia

successful trials of eliminating irradiation in the conditioning regimens even in recipients of BMT from unrelated donor have been achieved [8–11]. Subsequently, alternative regimens have been developed to reduce the potential risk of irradiation and GVHD using a non-irradiation based preparative therapy including a low-dose CY, FLU and ATG [6–8, 10]. Here, we showed that BMT using FLU-based reduced-intensity conditioning regimens led to improvement of the outcome for FA patients regardless of the donor type. In line with our findings, other investigators reported that HSCT using FLU-containing regimens was associated with a better outcome even for recipients of allograft from unrelated donor with stable engraftment and minimal toxicity, whereas adding ATG to the conditioning regimen contributed to decreasing the incidence of GVHD [7, 8, 11, 12]. On the other hand, it was reported that bone marrow recipients from unrelated donor showed less successful transfusion rate with high percentage of graft failure and RRT compared to bone marrow recipients from related donor [13]. In our cohort, FLU/ATG/low-dose CY-based conditioning regimen was tolerable and efficient for FA patients even for BM recipient from unrelated (HLA-1 locus mismatched) donor, but some patients developed virus reactivation such as CMV, BKV and EBV. To overcome virus reactivation that might occur as an adverse event following the use of ATG-containing regimen, it is better to decrease the ATG dose from 10 to 5 mg/kg. FA patients are more prone to cancer development such as squamous cell carcinomas with special predilection sites (esophagus, head and neck) [4, 14, 15]. FLU-containing regimens were employed in a limited number of FA patients, making it difficult to speculate on its implications on cancer progression. Three out of four patients received HSCT from HLA-matched related donor without irradiation and they showed successful and excellent outcomes. Therefore, it is important to consider the use of the conditioning regimen without irradiation for this group of patients. Several studies have demonstrated that TBI with 300–450 cGY is needed for consistent engraftment in recipients from unrelated donor [12, 16]. We would like to emphasize that reduction of irradiation dose in the conditioning regimens even for recipients of HSCT from unrelated donor is an important target that will improve the patient's quality of life by reducing late effects, particularly the risk of malignancy. Noteworthy, in our series three out of eight patients were asymptomatic. Although our findings were consistent with other investigators' results [3–5], early diagnosis and optimal timing of transplant in

asymptomatic FA patients is challenging and it is of utmost importance to confirm FA diagnosis in those patients who might be misdiagnosed with acquired aplastic anemia. In conclusion, the identification of asymptomatic FA patients requires careful consideration by testing for cross-linker hypersensitivity that provides a reliable cellular marker for FA diagnosis. HSCT using FLU/low-dose CY/ATG-based regimen is beneficial and could be a promising therapeutic approach for FA patients regardless of the donor type with favorable clinical outcome.

Acknowledgments This work was supported in part by grant for scientific research by the Ministry of Education, Culture, Sports, Science and Technology, Japan.

Conflict of interest The authors declare no conflict of interest.

References

1. Fanconi G. Familial constitutional panmyelocytopathy, Fanconi's anemia (F.A.). I. Clinical aspects. Semin Hematol. 1967;4: 233–40.
2. Alter BP. Fanconi's anemia and malignancies. Am J Hematol. 1996;53:99–110.
3. Kutler DI, Singh B, Satagopan J, Batish SD, Berwick M, Giampietro PF, Hanenberg H, Auerbach AD. A 20-year perspective on the International Fanconi Anemia Registry (IFAR). Blood. 2003;101:1249–56.
4. Shimamura A, Alter BP. Pathophysiology and management of inherited bone marrow failure syndromes. Blood Rev. 2010;24: 101–22.
5. Auerbach AD. Fanconi anemia and its diagnosis. Mutat Res. 2009;668:4–10.
6. Yabe M, Yabe H, Hamanoue S, Inoue H, Matsumoto M, Koike T, Ishiguro H, Morimoto T, Arakawa S, Ohshima T, Masukawa A, Miyachi H, Yamashita T, Katob S. In vitro effect of fludarabine, cyclophosphamide, and cytosine arabinoside on chromosome breakage in Fanconi anemia patients: relevance to stem cell transplantation. Int J Hematol. 2007;85(4):354–61.
7. Yabe H, Inoue H, Matsumoto M, Hamanoue S, Koike T, Ishiguro H, Koike H, Suzuki K, Kato S, Kojima S, Tsuchida M, Mori T, Adachi S, Tsuji K, Koike K, Morimoto A, Sako M, Yabe M. Allogeneic haematopoietic cell transplantation from alternative donors with a conditioning regimen of low-dose irradiation, fludarabine and cyclophosphamide in Fanconi anaemia. Br J Haematol. 2006;134:208–12.
8. MacMillan ML, Wagner JE. Haematopoietic cell transplantation for Fanconi anaemia—when and how? Br J Haematol. 2010; 149:14–21.
9. Gluckman E, Berger R, Dutreix J. Bone marrow transplantation for Fanconi anemia. Semin Hematol. 1984;21:20–6.
10. Kapelushnik J, Or R, Slavin S, Nagler A. A fludarabine-based protocol for bone marrow transplantation in Fanconi's anemia. Bone Marrow Transplant. 1997;20:1109–10.
11. Dalle JH. HSCT for Fanconi anemia in children: factors that influence early and late results. Bone Marrow Transplant. 2008; 42:S51–3.
12. Chaudhury S, Auerbach AD, Kernan NA, Small TN, Prockop SE, Scaradavou A, Heller G, Wolden S, O'Reilly RJ, Boulad F. Fludarabine-based cytoreductive regimen and T-cell-depleted grafts from alternative donors for the treatment of high-risk patients with Fanconi anaemia. Br J Haematol. 2008;140:644–55.
13. Gluckman E, Auerbach AD, Horowitz MM, Sobocinski KA, Ash RC, Bortin MM, Butturini A, Camitta BM, Champlin RE, Friedrich W, Good RA, Gordon-Smith EC, Harris RE, Klein JP, Ortega JJ, Pasquini R, Ramsay NK, Speck B, Vowels MR, Zhang MJ, Gale RP. Bone marrow transplantation for Fanconi anemia. Blood. 1995;86:2856–62.
14. Rosenberg PS, Socié G, Alter BP, Gluckman E. Risk of head and neck squamous cell cancer and death in patients with Fanconi anemia who did and did not receive transplants. Blood. 2005;105: 67–73.
15. Masserot C, Peffault de Latour R, Rocha V, Leblanc T, Rigolet A, Pascal F, Janin A, Soulier J, Gluckman E, Socié G. Head and neck squamous cell carcinoma in 13 patients with Fanconi anemia after hematopoietic stem cell transplantation. Cancer. 2008;113:3315–22.
16. MacMillan ML, Blazar BR, DeFor TE, Dusenbery K, Wagner JE. Thymic shielding (TS) in recipients of total body irradiation (TBI) and alternative donor hematopoietic stem cell transplant (AD-HSCT): reduced risk of opportunistic infection in patients with Fanconi anemia (FA). Blood. 2006;108 (abstract #3134).

The EMBO Journal (2012) 00, 1–13 | © 2012 European Molecular Biology Organization | All Rights Reserved 0261-4189/12
www.embojournal.org

THE EMBO JOURNAL

Histone chaperone activity of Fanconi anemia proteins, FANCD2 and FANCI, is required for DNA crosslink repair

Koichi Sato[1,7], Masamichi Ishiai[2,7], Kazue Toda[1], Satoshi Furukoshi[1], Akihisa Osakabe[1], Hiroaki Tachiwana[1], Yoshimasa Takizawa[1], Wataru Kagawa[1], Hiroyuki Kitao[2,3], Naoshi Dohmae[4], Chikashi Obuse[5], Hiroshi Kimura[6], Minoru Takata[2,*] and Hitoshi Kurumizaka[1,*]

[1]Laboratory of Structural Biology, Graduate School of Advanced Science and Engineering, Waseda University, Tokyo, Japan, [2]Laboratory of DNA Damage Signaling, Department of Late Effects Studies, Radiation Biology Center, Kyoto University, Kyoto, Japan, [3]Graduate School of Medical Sciences, Department of Molecular Oncology, Kyushu University, Fukuoka, Japan, [4]RIKEN Advanced Science Institute, Saitama, Japan, [5]Graduate School of Life Science, Hokkaido University, Hokkaido, Japan and [6]Graduate School of Frontier Biosciences, Osaka University, Osaka, Japan

Fanconi anaemia (FA) is a rare hereditary disorder characterized by genomic instability and cancer susceptibility. A key FA protein, FANCD2, is targeted to chromatin with its partner, FANCI, and plays a critical role in DNA crosslink repair. However, the molecular function of chromatin-bound FANCD2-FANCI is still poorly understood. In the present study, we found that FANCD2 possesses nucleosome-assembly activity *in vitro*. The mobility of histone H3 was reduced in FANCD2-knockdown cells following treatment with an interstrand DNA crosslinker, mitomycin C. Furthermore, cells harbouring FANCD2 mutations that were defective in nucleosome assembly displayed impaired survival upon cisplatin treatment. Although FANCI by itself lacked nucleosome-assembly activity, it significantly stimulated FANCD2-mediated nucleosome assembly. These observations suggest that FANCD2-FANCI may regulate chromatin dynamics during DNA repair.

The EMBO Journal advance online publication, 24 July 2012; doi:10.1038/emboj.2012.197

Subject Categories: genome stability & dynamics; chromatin & transcription

Keywords: DNA repair; FANCD2; FANCI; Fanconi anaemia; histone chaperone

*Corresponding authors. M Takata, Laboratory of DNA Damage Signaling, Radiation Biology Center, Kyoto University, Yoshida-konoe, Sakyo-ku, Kyoto 606-8501, Japan. Tel.: +81 75 753 7563; Fax: +81 75 753 7565; E-mail: mtakata@house.rbc.kyoto-u.ac.jp
or H Kurumizaka, Laboratory of Structural Biology, Graduate School of Advanced Science and Engineering, Waseda University, 2-2 Wakamatsu-cho, Shinjuku-ku, Tokyo 162-8480, Japan. Tel.: +81 3 5369 7315; Fax: +81 3 5367 2820; E-mail: kurumizaka@waseda.jp
[7]These authors contributed equally to this work

Received: 17 June 2012; accepted: 3 July 2012

Introduction

Fanconi anaemia (FA) is a rare hereditary disorder characterized by skeletal abnormalities, progressive bone marrow failure, and genomic instability accompanied by cancer susceptibility (Venkitaraman, 2004; Niedernhofer *et al*, 2005; Taniguchi and D'Andrea, 2006; Wang, 2007). FA-mutant cells are highly sensitive to interstrand DNA crosslinking reagents, which induce stalled replication forks, suggesting that FA proteins promote the stabilization and restarting of the replisome (Thompson *et al*, 2005; Wang, 2007).

Thirteen genes, *FANCA*, *-B*, *-C*, *-D1* (*BRCA2*), *-D2*, *-E*, *-F*, *-G*, *-I*, *-J* (*BRIP1*), *-L*, *-M*, and *-N* (*PALB2*), corresponding to individual FA complementation groups, have been cloned (Thompson *et al*, 2005; Wang, 2007; Kee and D'Andrea, 2010; Garner and Smogorzewska, 2011; Kitao and Takata, 2011). In addition, homozygous Rad51C mutations have recently been identified in a family with an FA-like disorder, as the *FANCO* gene (Vaz *et al*, 2010), and *SLX4* has been confirmed as the *FANCP* gene (Crossan *et al*, 2011; Kim *et al*, 2011; Stoepker *et al*, 2011). These FA gene products constitute a common DNA damage response pathway that is often referred to as the 'FA pathway'. In this pathway, eight proteins, FANCA, -B, -C, -E, -F, -G, -L, and -M, and three FANCA-associated polypeptides (FAAPs) form the FA core E3 ligase complex (Garcia-Higuera *et al*, 2001; Wang, 2007; Ali *et al*, 2012; Kim *et al*, 2012; Leung *et al*, 2012). On the other hand, FANCD2 and FANCI associate with each other to form a different complex, called the ID complex (Sims *et al*, 2007; Smogorzewska *et al*, 2007).

Upon DNA damage during S-phase, multiple phosphorylations of FANCI trigger the monoubiquitination of FANCD2 and FANCI by the FA core complex (Ishiai *et al*, 2008). The monoubiquitinated ID complex is then targeted to the chromatin, where it plays a critical role in DNA-repair pathways, such as homologous recombination and translesion synthesis (Matsushita *et al*, 2005; Thompson *et al*, 2005; Yamamoto *et al*, 2005; Wang, 2007; Kee and D'Andrea, 2010; Garner and Smogorzewska, 2011; Kitao and Takata, 2011). Recent studies indicated that monoubiquitinated FANCD2 (and FANCI) recruit the FAN1 nuclease, which possesses endo- and exonuclease activities, providing a partial explanation for their roles in DNA repair (Kratz *et al*, 2010; MacKay *et al*, 2010; Smogorzewska *et al*, 2010; Yoshikiyo *et al*, 2010). Monoubiquitinated FANCD2 also reportedly recruits SLX4 (Garner and Smogorzewska, 2011; Yamamoto *et al*, 2011), which is considered to function as a scaffold that interacts with the other nucleases, SLX1, XPF, and MUS81 (Fekairi *et al*, 2009; Svendsen *et al*, 2009; Yamamoto *et al*, 2011). Furthermore, a recent report found that FANCD2 itself might have exonuclease activity (Pace *et al*, 2010). However, whether chromatin-bound FANCD2 and FANCI have any additional functions remains to be determined.

The nucleosome is the fundamental repeating unit of chromatin (Wolffe, 1998). Four core histones, H2A, H2B,

H3, and H4, are the protein components of the nucleosome. H2A forms a specific dimer with H2B (H2A/H2B dimer), and H3 forms a specific dimer with H4 (H3/H4 dimer). During nucleosome assembly, two H3/H4 dimers (H3/H4 tetramer) are first deposited on DNA, forming a tetrasome, in which the DNA is wrapped around the H3/H4 tetramer. Two H2A/H2B dimers are then incorporated into the tetrasome to form the mature nucleosome, in which about 150 base pairs of DNA are wrapped around a histone octamer, containing two each of the H2A/H2B and H3/H4 dimers. In cells, nucleosomes are dynamically assembled and disassembled during the replication, transcription, recombination, and repair processes, and such nucleosome dynamics are accomplished with the aid of histone chaperones and/or ATP-dependent chromatin remodelling factors (Avvakumov *et al*, 2011).

In the present study, we purified the human and chicken FANCD2 proteins, and found that FANCD2 possesses nucleosome-assembly activity *in vitro*. We also purified FANCI, and showed that it significantly stimulated FANCD2-mediated nucleosome assembly, although FANCI itself lacked nucleosome-assembly activity. A histone-binding domain was mapped in the chicken FANCD2 C-terminal region (residues 1268–1439). The FANCD2 mutants, in which either the histone-binding domain was deleted or the Arg1336 and Lys1346 residues were replaced by Ala, were significantly defective in nucleosome assembly *in vitro*, and cells bearing these mutants displayed impaired survival upon cisplatin treatment *in vivo*. Furthermore, a disease-related mutation, human FANCD2(R302W) (Timmers *et al*, 2001), compromised histone dynamics, and the corresponding chicken FANCD2(R305W) also showed impaired histone chaperone activity. These data suggest that the histone chaperone activity of FANCD2 is crucial for the histone dynamics and the DNA crosslink repair in cells.

Results

Human FANCD2 promotes nucleosome assembly

In a proteome analysis to search for proteins in HeLa cell extracts that bind to the histone H3/H4 complex (Supplementary Figure S1), we unexpectedly detected human FANCD2 (hFANCD2) as a candidate interacting protein. Indeed, hFANCD2 was efficiently captured from a HeLa cell extract, using H3/H4 beads (Figure 1A). We purified hFANCD2 as a recombinant protein expressed in insect cells (Supplementary Figure S2A), and confirmed that purified hFANCD2 also bound to H3/H4 (Figure 1B). The hFANCD2-H3/H4 binding was also detected in the presence of DNaseI (Figure 1B, lane 5), indicating that the interaction is not mediated by DNA contamination. These results indicated that hFANCD2 directly binds to H3/H4, which prompted us to examine its nucleosome-assembly activity.

We tested hFANCD2-mediated nucleosome assembly by a topological assay, using relaxed circular DNA in the presence of topoisomerase (Figure 1C). The extent of nucleosome formation was assessed by analysing the superhelicity of circular DNA fractionated through an agarose gel, because negative supercoils are introduced when nucleosomes are formed. As shown in Figure 1C, the number of superhelical turns in the DNA substrate increased with greater amounts of hFANCD2. The faster migration of the DNA substrate was not due to DNA degradation (Supplementary Figure S2B). Therefore, hFANCD2 actually promoted nucleosome assembly *in vitro*. We next performed the nucleosome-assembly assay with a short DNA fragment, to directly detect the nucleosomes by an electrophoretic mobility shift assay. hFANCD2 stimulated the nucleosome assembly in this assay (Figure 1D, lanes 6–9). The nucleosome-assembly activity of hFANCD2 was slightly lower than that of human Nap1, which is a prominent nucleosome-assembly protein (Figure 1D). These biochemical results suggest that FANCD2 may regulate chromatin reorganization during DNA repair in higher eukaryotes.

Chromatin-bound FANCD2 is known to be monoubiquitinated, and the ubiquitin moiety may function to recruit its associated nucleases (Fekairi *et al*, 2009; Svendsen *et al*, 2009; Kratz *et al*, 2010; MacKay *et al*, 2010; Smogorzewska *et al*, 2010; Yoshikiyo *et al*, 2010; Yamamoto *et al*, 2011). Therefore, we tested whether FANCD2 monoubiquitination affects the nucleosome-assembly activity. For this purpose, we utilized the chicken FANCD2 protein (cFANCD2) (Yamamoto *et al*, 2005), which was bacterially expressed and purified to homogeneity (Supplementary Figure S2C). We then prepared monoubiquitinated cFANCD2, using purified components for the conjugation (i.e., FANCL, UBE2T, E1, and ubiquitin; Supplementary Figure S2D–F). As we previously reported, the cFANCD2 monoubiquitination was robustly enhanced in the presence of DNA (Sato *et al*, 2012), and about 40% of cFANCD2 was monoubiquitinated in this study (Supplementary Figure S2F). This monoubiquitinated cFANCD2 fraction was purified, and was subjected to the topological assay. However, we did not find a clear difference in the nucleosome-assembly activities between the fractions containing monoubiquitinated cFANCD2 and the monoubiquitination-deficient cFANCD2(K563R) mutant (Supplementary Figure S2G). Therefore, the monoubiquitination does not affect the activity. However, this could be due to the incomplete monoubiquitination of cFANCD2. Therefore, we prepared the monoubiquitination-mimicking version of FANCD2, by genetically fusing FANCD2(K563R) with ubiquitin to create FANCD2(K563R)-Ub (Supplementary Figure S2H), which is known to complement the DNA-repair-defective phenotype in the *FANCD2*$^{-/-}$ DT40 cells (Matsushita *et al*, 2005). We found that purified FANCD2(K563R)-Ub possessed similar histone-binding and nucleosome-assembly activities to those of cFANCD2 (Supplementary Figure S2I and J). These results suggested that the FANCD2 monoubiquitination may not be directly involved in the nucleosome assembly.

The C-terminal region of FANCD2 is responsible for interacting with histone H3/H4 and for promoting nucleosome assembly

To gain further insights into the molecular mechanism and the functional relevance of the nucleosome-assembly activity of FANCD2, we first searched for the FANCD2 region that interacts with the H3/H4 complex. We subjected cFANCD2 to limited proteolysis, and two fragments, cFANCD2(1-1167) and cFANCD2(1-1389), were identified (Figure 2A). These fragments lacked the acidic region, which is composed of the C-terminal 50 amino-acid residues of FANCD2. In addition, FANCD2(1268X), which also lacks the C-terminal region, is present in FA patients (FA Mutation Database, http://www.rockefeller.edu/fanconi/mutate/), suggesting the functional

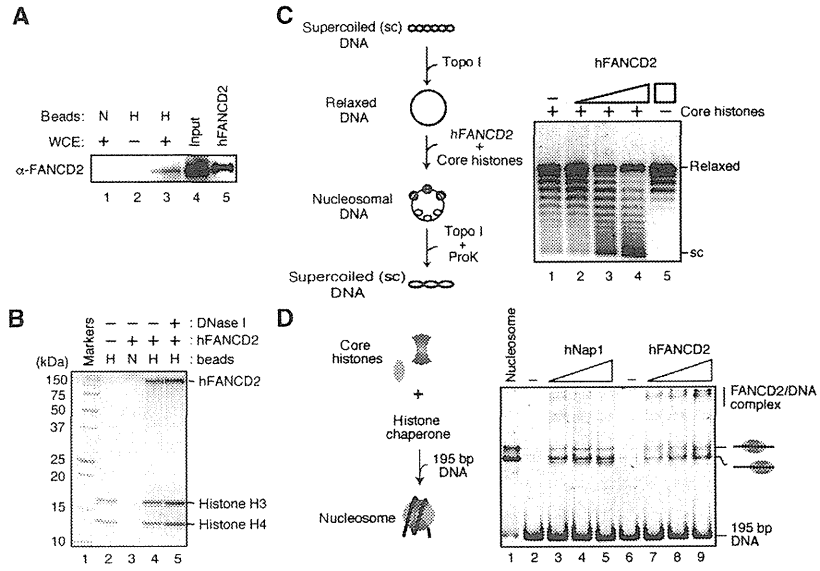

Figure 1 hFANCD2 promotes nucleosome assembly. (**A**) The H3/H4-conjugated beads were incubated with a HeLa WCE, and the endogenous FANCD2 bound to the beads was detected by western blotting with an anti-FANCD2 monoclonal antibody (α-FANCD2). N and H indicate the control Affi-Gel 10 beads and the H3/H4-conjugated beads, respectively. Input WCE (30 μg of protein) and hFANCD2 (125 ng) were applied in lanes 4 and 5, respectively. (**B**) The H3/H4 beads were incubated with purified hFANCD2 in the absence or presence of DNaseI, washed with buffer, and mixed with two-fold SDS sample buffer. The proteins bound to the beads were analysed by 15% SDS–PAGE. (**C**) Topological assay. A schematic diagram of topological assay is shown in the left panel. Nucleosomes were reconstituted on the relaxed plasmid DNA by hFANCD2 (0.2, 0.5, and 0.9 μM), in the presence of wheat germ topoisomerase I. After deproteinization, the topoisomers were separated by agarose gel electrophoresis. Highly supercoiled and relaxed DNAs are denoted as 'sc' and 'relaxed', respectively. (**D**) Nucleosome-assembly assay. A schematic diagram of the nucleosome-assembly assay is shown in the left panel. Nucleosomes were reconstituted on the linear 195 base-pair DNA by hNap1 (0.4, 0.8, and 1.6 μM) or hFANCD2 (0.2, 0.4, and 0.8 μM). Nucleosomes positioned at the edge and centre of the 195-bp DNA are indicated by cartoons on the right side of the panel.

importance of the FANCD2 C-terminal region. As histone chaperones are generally acidic, we investigated whether this acidic C-terminal region is essential for histone binding. The C-terminal deletion mutants, cFANCD2(1-1167), cFANCD2 (1-1267), and cFANCD2(1-1389), were expressed as GFP-tagged forms in HEK293T cells, and their H3/H4-binding activity was examined by a pull-down assay, using the H3/H4 beads. We found that cFANCD2(1-1167) and cFANCD2(1-1267) displayed diminished H3/H4 binding (Figure 2B, lanes 3 and 4). In contrast, cFANCD2(1-1389) retained residual H3/H4-binding activity (Figure 2B, lane 2). Consistently, cFANCD2(1-1167) and cFANCD2(1-1267) showed significant defects in nucleosome assembly (Figure 2C, lanes 13–17 and 18–22, and D; Supplementary Figure S3A). cFANCD2(1-1389) was completely proficient in the nucleosome-assembly activity under low protein concentration conditions (Figure 2C, lanes 8–12, and D; Supplementary Figure S3B). These observations suggest that the C-terminal region of FANCD2 (amino acids 1268–1389) is important for interacting with H3/H4 and for promoting nucleosome assembly. It should be noted that cFANCD2(1-1389) was defective in nucleosome assembly under high protein concentration conditions (Figure 2C, lanes 10–11, and D; Supplementary Figure S3C). This may reflect the biochemical property of cFANCD2(1-1389), which tends to form large protein–DNA aggregates that are unable to enter an agarose gel during electrophoresis (Supplementary Figure S3D).

Since the cFANCD2 C-terminal deletion may induce the improper folding of the cFANCD2 structure, we next performed the H3/H4-binding and nucleosome-assembly experiments with cFANCD2 point mutants. Based on the amino-acid conservation among the human, mouse, chicken, frog, fish, and fly FANCD2 proteins, we mutated the conserved amino-acid residues, which might be functionally important (Figure 2A). We found that the FANCD2(R1336A/K1346A) mutant, in which the Arg1336 and Lys1346 residues are replaced by Ala, was significantly defective in nucleosome assembly *in vitro*, while another mutant, cFANCD2(D1350A/E1365A/E1382A), in which the Asp1350, Glu1365, and Glu1382 residues are replaced by Ala, did not affect the nucleosome-assembly activity (Figure 2A, E, and F; Supplementary Figure S3E). Consistently, the histone-binding activity was substantially reduced in cFANCD2(R1336A/K1346A) (Figure 2B lane 11), but not in cFANCD2(D1350A/E1365A/E1382A) (Figure 2B, lane 10). These results strongly support the conclusion that FANCD2 promotes nucleosome assembly through its C-terminal histone-binding domain.

Finally, we tested the histone binding of the C-terminal cFANCD2 fragments, cFANCD2(669-1439) and cFANCD2 (953-1439), which contain the C-terminal amino-acid residues 669-1439 and 953-1439, respectively (Figure 2A). These cFANCD2 fragments were identified by a protease mapping experiment. As expected, the cFANCD2(669-1439) and cFANCD2(953-1439) fragments both efficiently bound to histones (Figure 2B, lanes 5 and 6). Surprisingly, cFANCD2 (953-1439), which contained only one-third of cFANCD2, promoted nucleosome assembly (Figure 2C, lanes 23–27, and D). Therefore, we concluded that the histone-binding domain is located in the C-terminal region of FANCD2.

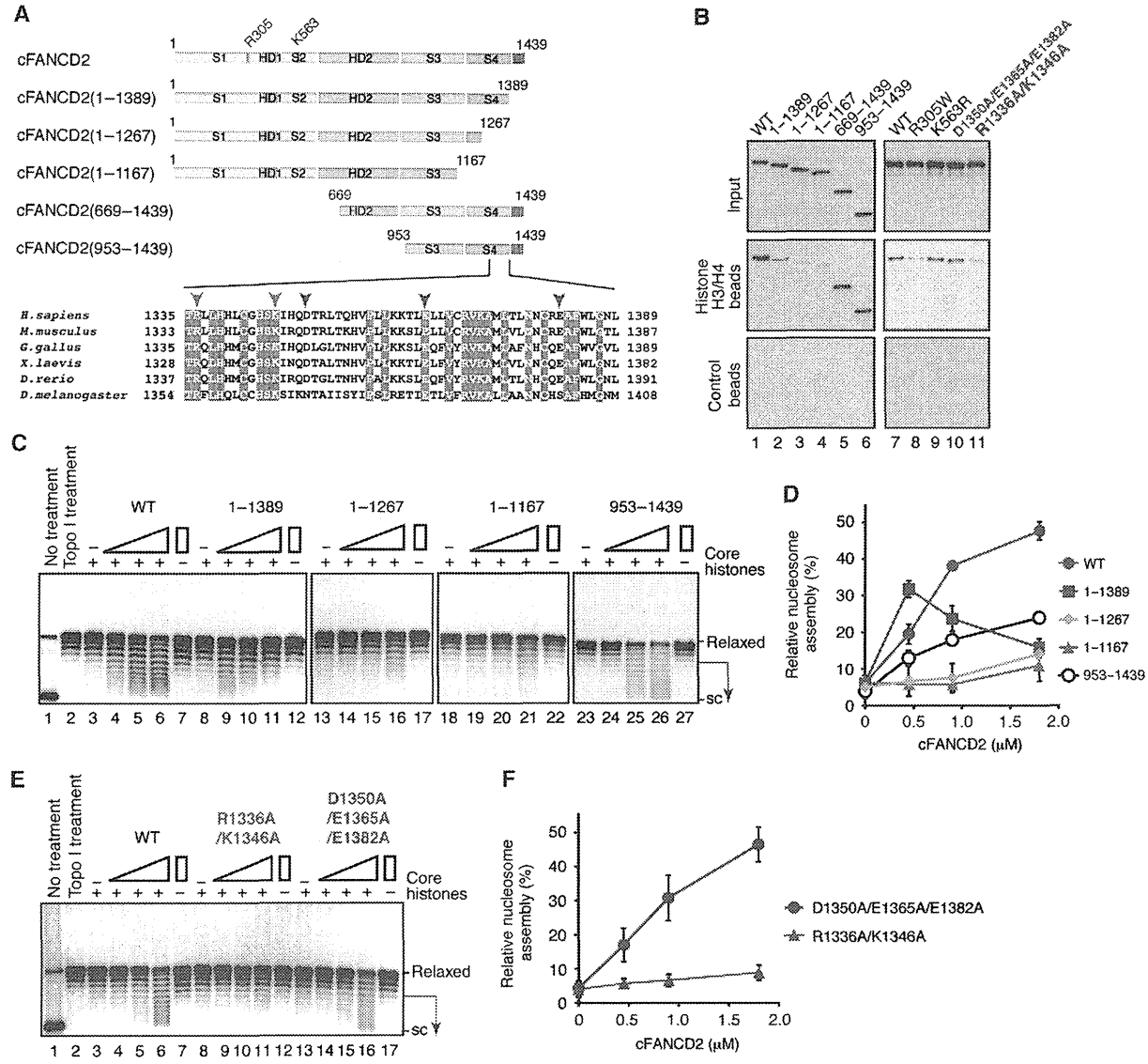

Figure 2 The C-terminal region of FANCD2 is responsible for histone binding and nucleosome assembly. (**A**) Schematic representations of full-length cFANCD2, and the cFANCD2(1-1389), cFANCD2(1-1267), cFANCD2(1-1167), cFANCD2(669-1439), and cFANCD2(953-1439) deletion mutants. The cFANCD2 domains, solenoid 1, helical domain 1, solenoid 2, helical domain 2, solenoid 3, and solenoid 4, are denoted as S1, HD1, S2, HD2, S3, and S4, respectively (Joo *et al*, 2011). The FANCD2 C-terminal acidic region is coloured red. The amino-acid sequences of the C-terminal regions of the *Homo sapiens*, *Mus musculus*, *Gallus gallus*, *Xenopus laevis*, *Danio rerio*, and *Drosophila melanogaster* FANCD2 proteins are aligned. The highly conserved residues are coloured red. The mutated residues in cFANCD2(R1336A/K1346A) and cFANCD2(D1350A/E1365A/E1382A) are indicated by orange and purple arrowheads, respectively. (**B**) The H3/H4 beads were incubated with extracts of HEK293T cells, producing either GFP-tagged cFANCD2, cFANCD2(1-1389), cFANCD2(1-1267), cFANCD2(1-1167), cFANCD2(669-1439), cFANCD2(953-1439), cFANCD2(R305W), cFANCD2(K563R), cFANCD2(D1350A/E1365A/E1382A), or cFANCD2(R1336A/K1346A). Proteins bound to the beads were detected by western blotting with an anti-chFANCD2 (polyclonal) antibody. The bottom panel indicates negative control experiments with beads lacking histones. (**C**) Nucleosomes were reconstituted on the relaxed plasmid DNA by cFANCD2 (lanes 3–7), cFANCD2(1-1389) (lanes 8–12), cFANCD2(1-1267) (lanes 13–17), cFANCD2(1-1167) (lanes 18–22), and cFANCD2(953-1439) (lanes 23–27) in the presence of wheat germ topoisomerase I. After deproteinization, the topoisomers were separated by agarose gel electrophoresis with ethidium bromide staining. The cFANCD2 concentrations were 0, 0.45, 0.90, and 1.8 μM. Highly supercoiled and relaxed DNAs are denoted as 'sc' and 'relaxed', respectively. (**D**) Graphic representation of nucleosome-assembly activities of the cFANCD2 mutants shown in **C**. Representative images are shown in **C**. The supercoiled DNA fractions were generated by nucleosome assembly in the presence of cFANCD2, and the intensities of the bands indicated by the arrows in **C** were quantitated by an LAS-4000 Image Analyser (GE Healthcare). Means of three independent experiments are shown with s.d.'s. (**E**) Nucleosomes were reconstituted on the relaxed plasmid DNA by cFANCD2 (lanes 3–7), cFANCD2(R1336A/K1346A) (lanes 8–12), and cFANCD2(D1350A/E1365A/E1382A) (lanes 13–17) in the presence of wheat germ topoisomerase I. The cFANCD2 concentrations were 0, 0.45, 0.90, and 1.8 μM. Highly supercoiled and relaxed DNAs are denoted as 'sc' and 'relaxed', respectively. (**F**) Graphical representation of the nucleosome-assembly activities of the cFANCD2 mutants shown in **E**. Representative images are shown in **E**. The supercoiled DNA fractions were generated by nucleosome assembly in the presence of cFANCD2, and the intensities of the bands indicated by the arrows in **E** were quantitated by an LAS-4000 Image Analyser (GE Healthcare). Means of three independent experiments are shown with s.d.'s.

FANCD2 mediates histone mobilization in living cells in a DNA damage-dependent manner

To determine whether FANCD2 plays a role in histone dynamics in living cells during DNA repair, we knocked down hFANCD2 in HeLa cells expressing histone H3-GFP (Kimura and Cook, 2001), using small inhibitory RNA (siRNA). Three days after the transfection of the specific siRNA, the level of hFANCD2 had decreased substantially, to <10% of the normal level (Supplementary Figure S4A and B). Using these cells, the mobility of H3 was analysed by fluorescence recovery after photobleaching (FRAP) (Kimura *et al*, 2006). The recovery kinetics (the curve shapes) of the exchanging fractions were similar in the hFANCD2-knockdown and control cells (Figure 3A), suggesting that hFANCD2 does not play a major role in H3 assembly or exchange under normal conditions. As FA-mutant cells display significant sensitivity to interstrand DNA crosslinking reagents, such as mitomycin C (MMC) (Niedernhofer *et al*, 2005; Thompson *et al*, 2005; Wang, 2007; Kee and D'Andrea, 2010; Garner and Smogorzewska, 2011; Kitao and Takata, 2011), we next tested the effect of MMC on the H3 mobility in the hFANCD2-knockdown HeLa cells. Interestingly, the recovery of H3-GFP in the hFANCD2-knockdown cells was clearly slower in the presence of MMC (Figure 3B). Similar results were obtained with a different FANCD2-specific siRNA (Supplementary Figure S4C). The slower H3-GFP exchange observed in the MMC-treated FANCD2-knockdown cells could be due to a different cell cycle distribution, since the FA-deficient cells may be arrested at S and/or G2 due to the deficiency of DNA crosslink repair. We therefore performed FRAP experiments in cells stably expressing both H3-GFP and mCherry-tagged PCNA, which shows characteristic patterns representing replication and repair foci (Leonhardt *et al*, 2000). We first examined the mobility of H3-GFP in different cell cycle stages under the normal growth conditions. The H3-GFP mobility in PCNA foci-positive (S-phase) cells did not differ from that in PCNA foci-negative cells (Figure 3C). In the presence of MMC, the PCNA foci-positive cells were indeed enriched by the hFANCD2 knockdown, but the mobility of H3-GFP was still slower than that in the MMC-treated PCNA foci-positive control cells (Figure 3D; Supplementary Figure S4D). Therefore, the reduced histone H3 mobility in the MMC-treated hFANCD2-knockdown cells does not appear to be attributable to a difference in the cell cycle phase. Furthermore, the slower H3-GFP recovery in the presence of MMC was also detected in the hFANCA-knockdown cells, in which the damage-dependent focus formation of hFANCD2 on chromosomes was significantly inhibited (Supplementary Figure S4E–H). These data suggest that hFANCD2 may mediate nucleosome assembly and/or histone exchange in human cells, in a damage-dependent manner.

The C-terminal histone-binding region of FANCD2 is important for the DNA repair mediated by the FA pathway

To determine whether the histone assembly activity levels of the FANCD2 mutants *in vitro* correlate with their DNA-repair activities *in vivo*, we expressed them in *FANCD2*$^{-/-}$ DT40 cells, and exposed the cells to cisplatin in a colony survival assay. As shown in Figure 4A, full-length cFANCD2, cFANCD2(1-1389), and cFANCD2(D1350A/E1365A/E1382A) rescued the cisplatin-sensitive phenotype of the *cFANCD2*$^{-/-}$ cells, in contrast to cFANCD2(1-1167), cFANCD2(1-1267),

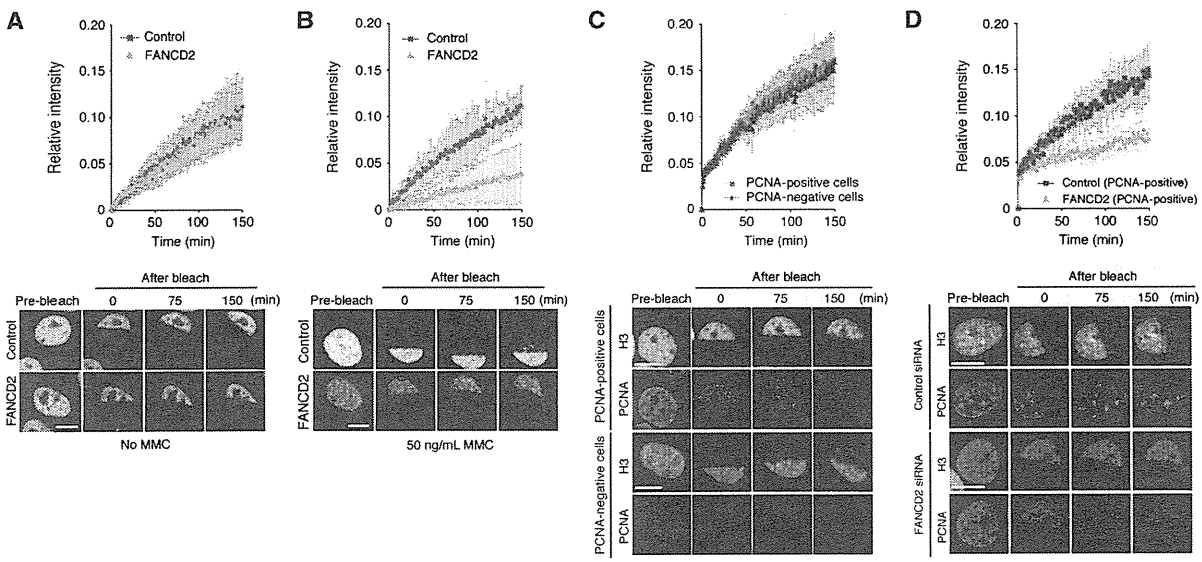

Figure 3 Histone H3 mobility is decreased in FANCD2-knockdown cells in the presence of a DNA crosslinking reagent. (**A**, **B**) FRAP with HeLa cells. Three days after the transfection of hFANCD2-siRNA or control RNA, the mobility of histone H3-GFP was analysed by bleaching one-half of a nucleus in the absence (**A**) or presence (**B**) of 50 ng/ml MMC for 12–18 h. The mean of the relative fluorescence intensity with the s.d. ($n = 10$–11) and examples are shown. (**C**) FRAP with HeLa cells stably expressing mCherry-PCNA. Three days after the transfection of control RNA, the mobility of histone H3-GFP was analysed in the absence of MMC. The PCNA foci-positive (S-phase) cells were identified by the characteristic mCherry-PCNA distribution. The mean of the relative fluorescence intensity with the s.d. ($n = 10$–14) and examples are shown. (**D**) FRAP with MMC-treated HeLa cells expressing H3-GFP and mCherry-PCNA in S-phase. Three days after the transfection of hFANCD2-siRNA or control RNA, the mobility of histone H3-GFP in the PCNA foci-positive (S-phase) cells was analysed in the presence of 50 ng/ml MMC. The mean of the relative fluorescence intensity with the s.d. ($n = 10$–18) and examples are shown. Bars: 10 μm.

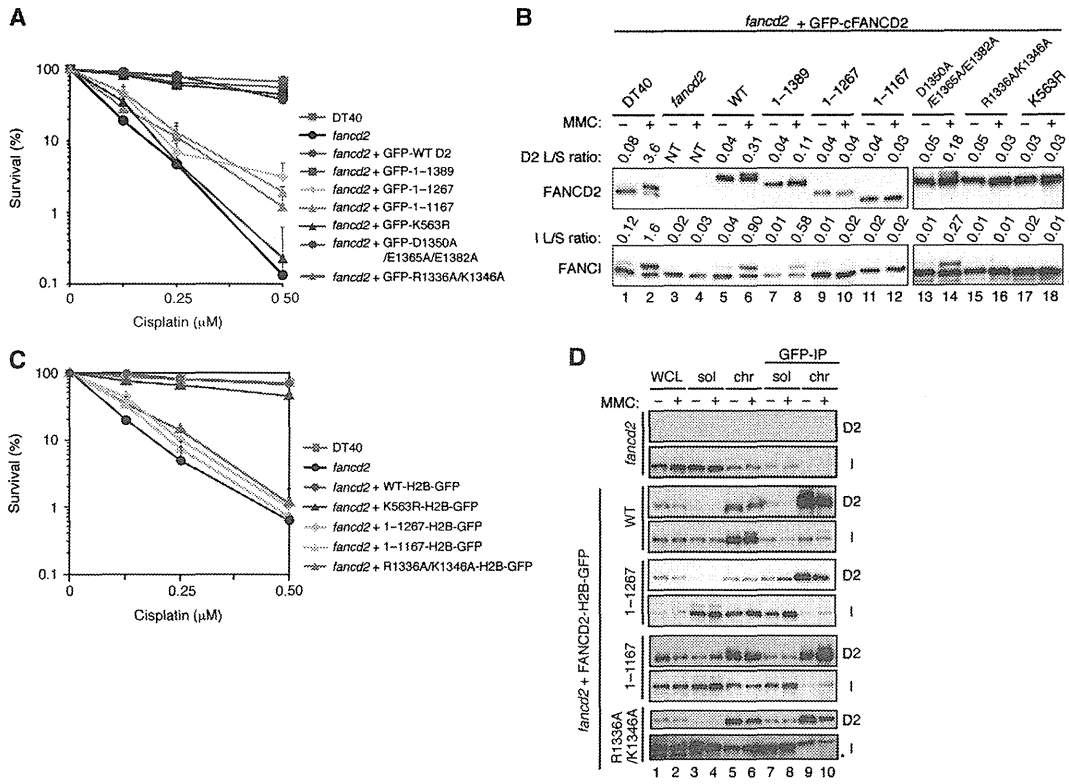

Figure 4 DNA-repair defects in the cFANCD2 C-terminal mutants. (**A**) Colony survival assay of the *cFANCD2*$^{-/-}$ DT40 cells expressing GFP fusions with the wild-type (WT) and indicated cFANCD2 mutants in the presence of cisplatin. The mean and s.d. of measurements performed in triplicate are shown. (**B**) FANCD2/FANCI monoubiquitination in *cFANCD2*$^{-/-}$ cells expressing the indicated cFANCD2 mutants. Cells were treated with or without MMC, and the WCEs were subjected to western blotting. The bands detected just above the original bands (S-forms) correspond to the monoubiquitinated forms (L-forms) of cFANCD2 and cFANCI (lanes 2, 6, 8, and 14). The L-form and S-form bands were quantitated with the Image J software, and the L/S ratios are indicated just above each panel. An asterisk indicates the non-specific bands. ND: not detectable. (**C**) Colony survival assay of the *cFANCD2*$^{-/-}$ cells expressing H2B-GFP fusions with the WT and indicated cFANCD2 mutants in the presence of cisplatin. The mean and s. d. of measurements performed in triplicate are shown. (**D**) Chromatin targeting of cFANCD2 (WT)-H2B, cFANCD2(1-1167)-H2B, cFANCD2(1-1267)-H2B, and cFANCD2(R1336A/K1346A)-H2B. Negative control experiments in the absence of exogenously expressed cFANCD2 are shown in the top panel. The *cFANCD2*$^{-/-}$ cells expressing the indicated proteins were treated with MMC (500 ng/ml, 6 h) or left untreated and then fractionated. Each fraction was separated by SDS–PAGE, and western blotting was performed using anti-cFANCD2 and anti-cFANCI antibodies. An asterisk indicates the non-specific band.

and cFANCD2(R1336A/K1346A). To ensure the chromatin targeting of these cFANCD2 mutants, we repeated this assay with the cFANCD2 mutants expressed as fusions with histone H2B, since cFANCD2(1-1167), cFANCD2(1-1267), and cFANCD2(R1336A/K1346A) were not monoubiquitinated (Figure 4B), probably due to the weakened interaction with FANCL, which was identified as the catalytic E3 subunit for FANCD2 monoubiquitination (Meetei *et al*, 2003) (Supplementary Figure S5A). We confirmed that the fusion of H2B to cFANCD2 and cFANCD2(1-1267) did not affect their nucleosome-assembly activities (Supplementary Figure S5B–E). Although substantial amounts of cFANCD2(1-1167)-H2B, cFANCD2(1-1267)-H2B, and cFANCD2(R1336A/K1346A)-H2B were detected at the chromatin (Figure 4D), the mutants still could not complement the cisplatin sensitivity of *cFANCD2*$^{-/-}$ cells, in contrast to the H2B fusion proteins with the full-length cFANCD2 and cFANCD2(K563R), bearing a point mutation at the monoubiquitination site (K563R) (Figure 4C) (Matsushita *et al*, 2005). These results strongly suggest that the nucleosome-assembly activity, which depends on the C-terminal region of FANCD2, might be crucial for the DNA repair mediated by the FA pathway. Notably, these cFANCD2 mutants were able to interact with the cFANCI protein in chromatin, as detected by anti-GFP immunoprecipitation followed by western blotting (Figure 4D), and as further supported by the results of *in vitro* binding experiments (Supplementary Figure S7F–H).

A disease-related FA mutant, human FANCD2(R302W), and its chicken counterpart, cFANCD2(R305W), are monoubiquitinated but do not facilitate histone exchange

As shown in Figure 4B, the C-terminally deleted or point FANCD2 mutants, which were defective in nucleosome assembly, were also defective in monoubiquitination, probably due to their weakened interactions with FANCL (Supplementary Figure S5A). This suggested that the histone-binding and FANCL-binding regions may partially overlap. To provide evidence that the FANCD2 histone-chaperone activity functions in DNA repair independently of its monoubiquitination, a FANCD2 mutant, in which the histone-chaperone and monoubiquitination activities are separated, would be useful.

We reasoned that such mutations might be found outside the putative histone-binding site. We found that the chicken FANCD2 R305W mutation (Arg305 to Trp), which corresponds to a disease-related mutation (human FANCD2 R302W) in FA (Timmers *et al*, 2001), is such a separation mutation. cFANCD2(R305W) exhibited reduced histone binding (Figure 2B, lane 8), and was defective in the nucleosome-assembly activity (Figure 5A and B). In contrast, cFANCD2(R305W) was proficient in its monoubiquitination (Figure 5C) and chromatin-targeting activities (Supplementary Figure S6A). Interestingly, cFANCD2(R305W) was moderately defective in the repair of DNA damage induced by cisplatin (Figure 5D), although its binding to cFANCI was proficient *in vivo* (Supplementary Figure S6A) and *in vitro* (Supplementary Figure S7E). The DNA-repair deficiency was also observed when H2B-fused cFANCD2(R305W) was expressed in the *cFANCD2*$^{-/-}$ cells (Figure 5E). These results indicated that the DNA-repair defect observed in the *cFANCD2*$^{-/-}$ cells expressing cFANCD2(R305W) may be accounted for by the defective histone chaperone activity of cFANCD2(R305W). Therefore, the histone chaperone activity of FANCD2 may be required in the steps after the FANCD2 monoubiquitination and chromatin targeting, during DNA repair by the FA pathway (Figure 8B).

To test whether the histone chaperone activity of FANCD2 functions in histone dynamics in living cells, we expressed mCherry-tagged hFANCD2, hFANCD2(R302W), or hFANCD2 (K561R) in H3-GFP-expressing HeLa cells, in which the endogenous hFANCD2 was knocked down by siRNA (Supplementary Figure S6B). We compared the H3-GFP mobility between mCherry-positive and -negative cells. The mobility of H3-GFP was efficiently restored with the expression of wild-type (WT) hFANCD2 (Figure 6A), but not with the monoubiquitination-deficient hFANCD2(K561R) mutant (Figure 6B, top panel), consistent with its chromatin-targeting deficiency (diffusing within the nucleus; Figure 6B, bottom panels). Interestingly, hFANCD2(R302W) also failed to restore the H3-GFP mobility (Figure 6C, top panel), although its chromatin targeting was not defective (forming nuclear foci like the WT hFANCD2; Figure 6C, bottom panels). Together with the DNA-repair deficiency of the *cFANCD2*$^{-/-}$ cells expressing cFANCD2(R305W), these results support the view that the histone-chaperone activity of FANCD2 is important in the DNA repair by the FA pathway. It should be noted that the VU008 patient cell line, which has the hFANCD2(R302W) mutation, produces the mutant hFANCD2 protein at extremely low levels (Timmers *et al*, 2001). Therefore, both defective histone-chaperone activity

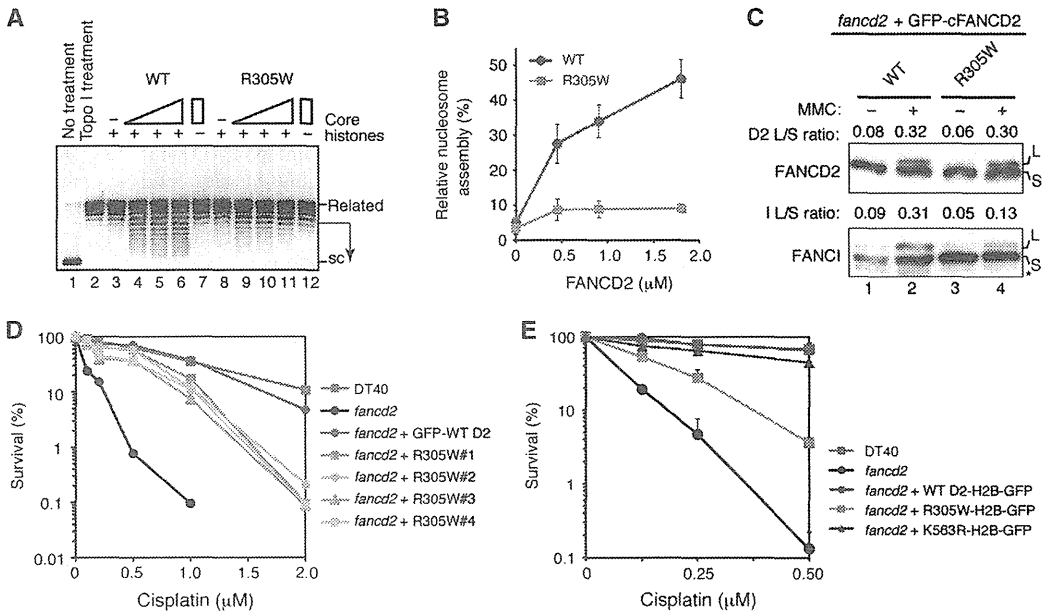

Figure 5 An FA-related mutant, cFANCD2(R305W), is defective in nucleosome-assembly activity and DNA repair. (**A**) Nucleosomes were reconstituted on the relaxed plasmid DNA by cFANCD2 (lanes 3–7) and cFANCD2(R305W) (lanes 8–12), in the presence of wheat germ topoisomerase I. After deproteinization, the topoisomers were separated by agarose gel electrophoresis. The cFANCD2 concentrations were 0, 0.45, 0.90, and 1.8 μM. Highly supercoiled and relaxed DNAs are denoted as 'sc' and 'relaxed', respectively. (**B**) Graphical representation of the nucleosome-assembly activity of the cFANCD2(R305W) mutants. Representative images are shown in **A**. The supercoiled DNA fractions were generated by nucleosome assembly in the presence of cFANCD2 (indicated by arrows in **A**), and the intensities of the bands indicated by the arrows in **A** were quantitated by an LAS-4000 Image Analyser (GE Healthcare). Means of three independent experiments are shown with s.d.'s. (**C**) FANCD2/FANCI monoubiquitination in *cFANCD2*$^{-/-}$ cells expressing the wild-type (WT) FANCD2 or cFANCD2(R305W). Cells were treated with or without MMC, and the WCEs were subjected to western blotting. The bands detected just above the original bands (S-forms) correspond to the monoubiquitinated forms (L-forms) of cFANCD2 and cFANCI (lanes 2 and 4). The L-form and S-form bands were quantitated with the Image J software, and the L/S ratios are indicated just above each panel. An asterisk indicates the non-specific band. (**D**) Colony survival assay of the cFANCD DT40 cells expressing GFP fusions with the wild type (WT) and cFANCD2(R305W), in the presence of cisplatin. Four independent DT40 cells expressing cFANCD2(R305W) were tested and plotted. (**E**) Colony survival assay of the *cFANCD2*$^{-/-}$ DT40 cells expressing H2B–GFP fusions with the WT and cFANCD2(R305W), in the presence of cisplatin. The mean and s.d. of measurements performed in triplicate are shown.

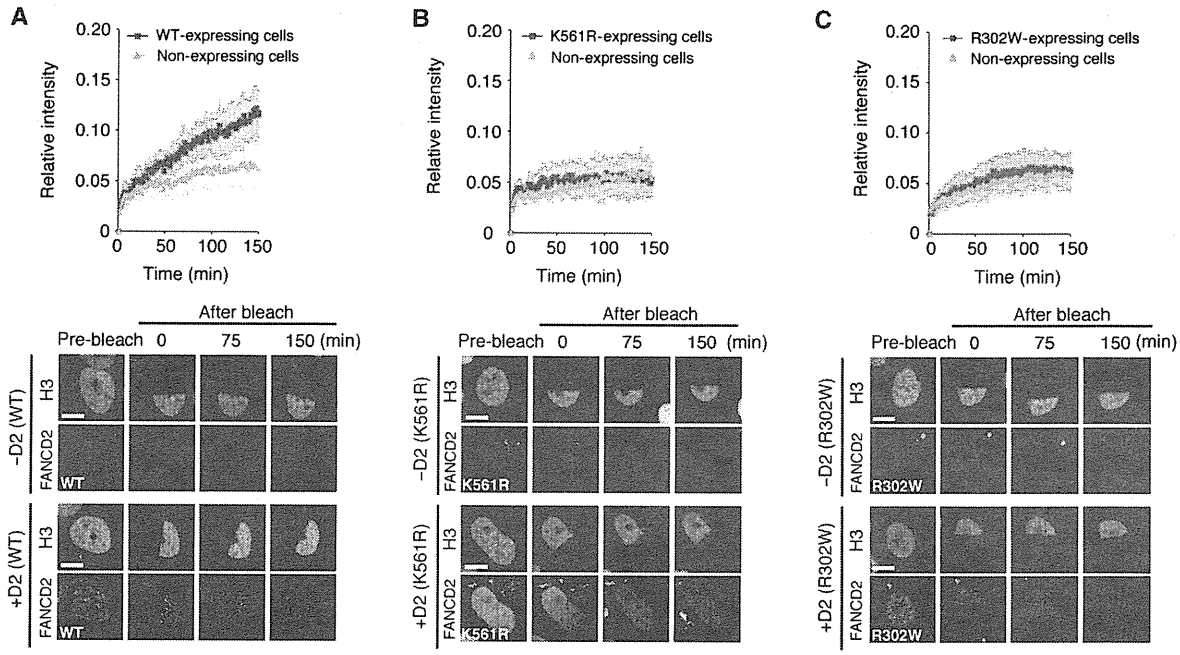

Figure 6 An FA-related mutant, human FANCD2(R302W), is defective in facilitating histone exchange. (**A–C**) FRAP with HeLa cells expressing H3-GFP and mCherry fusions with hFANCD2 (WT) (**A**), hFANCD2(K561R) (**B**), and hFANCD2(R302W) (**C**). After the depletion of endogenous hFANCD2 by siRNA, mCherry-hFANCD2, hFANCD2(K561R), or -hFANCD2(R302W) was expressed. In these cells, the mobility of histone H3-GFP was analysed in the presence of 50 ng/ml MMC for 12–18 h. The mean of the relative fluorescence intensity with the s.d. ($n = 10$–12) and examples are shown. Bars: 10 μm.

and instability of hFANCD2(R302W) protein may be potential causes of the FA phenotype in this patient.

FANCI stimulates nucleosome assembly by FANCD2

Finally, we examined the involvement of FANCI in nucleosome assembly, using purified chicken FANCI (cFANCI) (Supplementary Figure S7A and B), which could form a stable complex with cFANCD2 (Figure 7A). Although FANCI shares significant homology with FANCD2 (Sims *et al*, 2007; Smogorzewska *et al*, 2007), purified cFANCI alone did not efficiently promote nucleosome assembly (Figure 7B). However, cFANCI clearly stimulated the cFANCD2-mediated nucleosome assembly at low cFANCD2 concentrations, at which cFANCD2 itself did not promote detectable levels of nucleosome assembly (Figure 7C and D). cFANCI did not form a complex with the major histone chaperone Nap1, and did not stimulate its nucleosome assembly (Supplementary Figure S7C and D), suggesting that it may specifically stimulate the cFANCD2-mediated nucleosome assembly. In addition, cFANCI stimulated the nucleosome-assembly activity of cFANCD2(1-1389), which retained H3/H4-binding ability, but not that of cFANCD2(1-1267) (Supplementary Figure S7I). Therefore, the ID complex may facilitate nucleosome reorganization during DNA repair.

Discussion

In the present study, we found that the purified FANCD2 protein promotes nucleosome assembly *in vitro*, and that its partner, FANCI, significantly stimulates this activity. We also discovered that the C-terminal region of FANCD2 is critical for the nucleosome-assembly activity, and showed that the FANCD2 deletion and point mutants are defective in both nucleosome assembly *in vitro* and tolerance to cisplatin treatment *in vivo*. These findings provide novel insights into the function of the ID complex in chromatin.

The crystal structure of the mouse ID complex revealed that FANCD2 is composed of seven subdomains, solenoid 1 (S1), helical domain 1 (HD1), solenoid 2 (S2), helical domain 2 (HD2), solenoid 3 (S3), solenoid 4 (S4), and the C-terminal acidic region (Joo *et al*, 2011). In the present study, we mapped the histone-binding region within the S4 domain of FANCD2. The FANCD2 S4 domain is separate from the FANCI-binding surface, and is largely accessible (Joo *et al*, 2011). In the S4 domain, the cFANCD2 Arg1336 and Lys1346 residues are perfectly conserved among the human, mouse, chicken, frog, fish, and fly FANCD2 proteins (Figure 2A), and are located on the concave surface (Figure 8A; Joo *et al*, 2011). Our mutational analysis revealed that the cFANCD2 Arg1336 and Lys1346 residues are essential for nucleosome assembly *in vitro* and cisplatin resistance *in vivo*. In the crystal structure, the side chains of the mouse FANCD2 Arg1334 and Lys1344 residues, corresponding to the cFANCD2 Arg1336 and Lys1346 residues, respectively, are completely exposed to the solvent on the concave surface (Figure 8A). Therefore, the concave surface of the FANCD2 S4 domain may be its histone-binding region.

In cFANCD2, Arg1336 and Lys1346 are positively charged residues, which are considered to be less important for the histone binding of the acidic histone chaperone, Asf1 (English *et al*, 2006; Natsume *et al*, 2007). However, the involvement of positively charged residues in histone

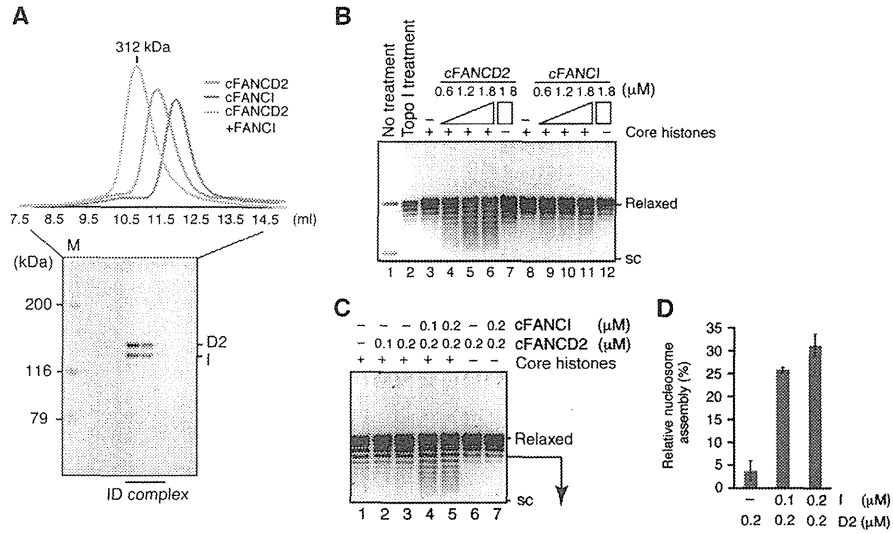

Figure 7 FANCI stimulates the FANCD2-mediated nucleosome assembly. (**A**) Gel filtration analysis of cFANCI–cFANCD2 complex formation. The SDS–PAGE analysis of the cFANCI–cFANCD2 fractions is shown below the gel filtration profiles. (**B, C**) Nucleosomes were reconstituted with relaxed plasmid DNA and cFANCD2 and/or cFANCI in the presence of wheat germ topoisomerase I. After deproteinization, the topoisomers were separated by agarose gel electrophoresis. The protein concentrations used in the assay are indicated at the top of the panels. Highly supercoiled and relaxed DNAs are denoted as 'sc' and 'relaxed', respectively. (**D**) Graphical representation of the experiments shown in **C**, lanes 3–5. The supercoiled DNA fractions generated by nucleosome assembly in the presence of cFANCD2 and cFANCI (indicated by arrows in **C**) were quantitated. Means of three independent experiments are shown with s.d.'s.

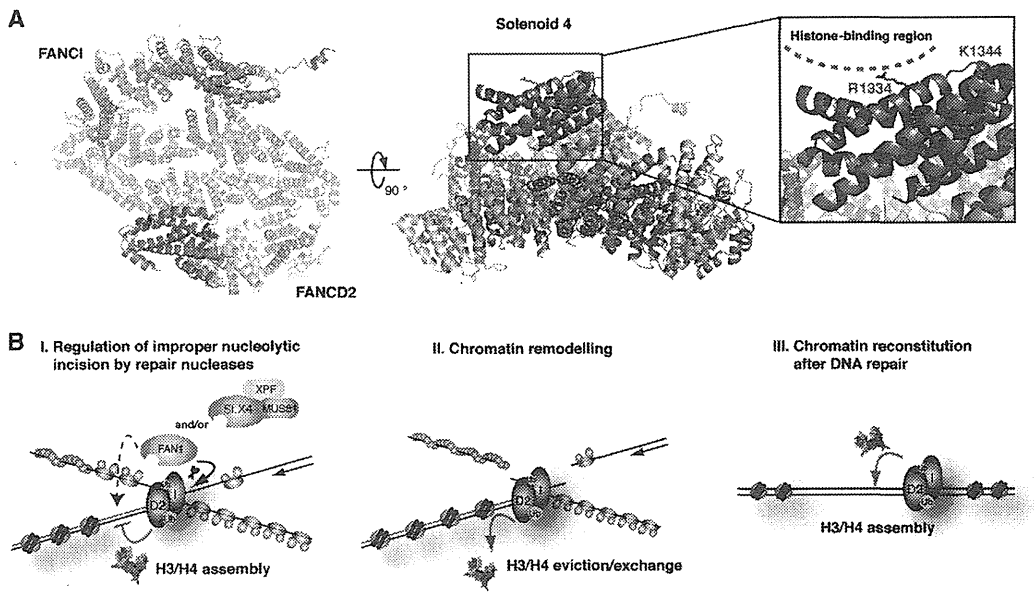

Figure 8 Models for the FANCD2 function in the FA pathway. (**A**) Locations of the Arg1334 and Lys1344 residues in the mouse FANCD2 structure. Structure of the mouse ID complex (PDB ID: 3S4W; Joo *et al*, 2011). The FANCD2 and FANCI subunits are coloured grey and light blue, respectively. The FANCD2 Arg1334 and Lys1344 residues (red), corresponding to the cFANCD2 Arg1336 and Lys1346 residues, respectively, are located on the concave surface of the FANCD2 Solenoid 4 (S4) domain (dark grey). (**B**) Three possible functions of the histone chaperone activity of the ID complex. (I) After the chromatin binding and monoubiquitination of the ID complex, the nucleosomes assembled by the ID complex on newly synthesized DNA may suppress the improper nucleolytic digestion by the repair nucleases, such as FAN1 and the SLX4 nuclease complex, which are recruited by the monoubiquitinated ID complex. (II) Chromatin remodelling mediated by the ID complex and FANCD2-associated chromatin modifiers may facilitate the RAD51-mediated homologous recombination reaction in chromatin. (III) The nucleosome-assembly activity of the ID complex may be required for chromatin reconstitution after DNA repair. RAD51 and RPA are coloured red and green, respectively. Histone octamers are shown in brown.

binding has been reported in the histone chaperone HJURP, which is the specific chaperone for the histone H3 variant, CENP-A (Dunleavy *et al*, 2009; Foltz *et al*, 2009). In the complex of HJURP with histone H4 and CENP-A, polar interactions exist between the negatively charged Glu96 of CENP-A and the two positively charged Arg32 and Lys39

residues of HJURP, and also between Glu107 of CENP-A and Arg28 of HJURP (Hu *et al*, 2011). Interestingly, the Glu96 and Glu107 residues of CENP-A are both conserved in histone H3 (Tachiwana *et al*, 2011a). Therefore, the histone-binding mechanism of FANCD2 may be similar to that of HJURP.

In the present study, we found that cFANCD2(R305W) was clearly defective in reversing the cisplatin sensitivity of the *FANCD2*$^{-/-}$ DT40 cells, but was proficient in its monoubiquitination *in vivo*. Interestingly, cFANCD2(R305W) was significantly defective in both the histone-binding and nucleosome-assembly activities. In addition, the corresponding human FANCD2(R302W) mutant could not rescue the decreased histone H3 mobility in the FANCD2-knockdown cells. These findings indicate that the histone-chaperone activity of FANCD2 is actually involved in the DNA crosslink repair by the FA pathway, and strongly suggest that FANCD2 regulates nucleosome dynamics after its monoubiquitination. The C-terminal cFANCD2 mutants tested in this study showed more severe cisplatin sensitivity than cFANCD2(R305W), even when localized in the chromatin by the H2B fusion. The residual histone-chaperone activity of cFANCD2 (R305W), which was barely detectable in the present nucleosome formation assay, may partially complement the cisplatin sensitivity of the *cFANCD2*$^{-/-}$ cells. In the crystal structure of mouse FANCD2, the side chain of the corresponding Arg300 directly hydrogen bonds with Asp379 (Joo *et al*, 2011), suggesting that the Arg300–Asp379 interaction may be important in the tertiary structure of the protein. Therefore, the Arg to Trp substitution found in cFANCD2(R305W) or hFANCD2(R302W) may cause a large structural change, which may allosterically impair the histone-binding activity of FANCD2.

FANCI–FANCD2 is reportedly required for nucleolytic incisions in a replicating plasmid carrying an interstrand crosslink in a frog egg extract (Knipscheer *et al*, 2009). One can envision that the ID complex-mediated chromatin remodelling may regulate the incision step by promoting the recruitment of nucleases (Figure 8B, I) (e.g., FAN1, Mus81, and XPF) (Nomura *et al*, 2007; Bhagwat *et al*, 2009; Fekairi *et al*, 2009; Svendsen *et al*, 2009; Hicks *et al*, 2010; Kratz *et al*, 2010; MacKay *et al*, 2010; Smogorzewska *et al*, 2010; Yoshikiyo *et al*, 2010; Yamamoto *et al*, 2011). In this step, the proper incision by the repair nucleases may occur on the single-stranded DNA region (Figure 8B, I, arrowhead), while the improper digestion of intact DNA strands may be restricted by the nucleosomes formed by the ID complex (Figure 8B, I, dashed line). Second, in the FA pathway, homologous recombination repair may be promoted after FANCD2 assembly into chromatin. The nucleosome remodelling by the ID complex may facilitate the DNA recombination reaction mediated by RAD51, which is the key protein for homologous recombinational repair (Figure 8B, II). Finally, the histone assembly activity of the ID complex may simply be important for chromatin reformation, following crosslink removal and DNA repair (Figure 8B, III). In addition to the direct interaction of the ID complex with histones, presented here, several chromatin modifiers have been suggested to interact with FA proteins. For example, a histone acetyltransferase, TIP60, reportedly interacts with FANCD2 (Hejna *et al*, 2008). Thus, the function of FANCD2 may be tightly coupled with those of other chromatin remodelling factors in chromatin dynamics, to facilitate DNA crosslink repair.

Materials and methods

Purifications of FANCD2, FANCI, FANCL, UBE2T, and Nap1

Experimental procedures are described in Supplementary Materials and Methods. The protein concentration was determined by the Bradford method (Bradford, 1976), using bovine serum albumin as the standard protein.

Purification of recombinant human H3/H4 and H2A/H2B complexes

Human histones H2A, H2B, H3, and H4 were overexpressed in *Escherichia coli* cells as His_6-tagged proteins, as described (Tanaka *et al*, 2004; Tachiwana *et al*, 2008). The purification and preparation of the histone H3/H4 and H2A/H2B complexes were performed as previously described (Tachiwana *et al*, 2010, 2011b). The His_6-tag was removed during the purification steps.

Proteome analysis

The purified recombinant human histone H3/H4 complex was covalently conjugated with Affi-Gel 10 beads (Bio-Rad), according to the manufacturer's protocol. Briefly, the histone H3/H4 beads were incubated with a chromatin extract from HeLa cells at 4°C. The beads were washed with 10 mM PIPES buffer (pH 7.0), containing 1 mM $MgCl_2$, 1 mM EDTA, 0.01% Triton X-100, 300 mM sucrose, and 0.1 M NaCl. The proteins bound to the beads were fractionated by SDS–PAGE. Each lane was cut into nine pieces, and was further treated with trypsin. To identify the peptide fragments, the samples were analysed by liquid chromatography/tandem mass spectrometry, as previously described (Nozawa *et al*, 2010). The raw data files were analysed by the Mascot software (Matrix Science).

Pull-down assay with histone-conjugated beads

The histone H3/H4 complex was covalently conjugated with Affi-Gel 10 beads (Bio-Rad), according to the manufacturer's protocol. The histone H3/H4 beads were incubated with a HeLa whole-cell extract (WCE) (3 mg of protein), and the beads were washed three times with 100 µl of washing buffer, containing 50 mM Tris–HCl (pH 7.5), 200 mM NaCl, 5 mM EDTA, 0.5% Nonidet P-40, 1 mM PMSF, and Protease Inhibitor Cocktail (Nacalai Tesque). The hFANCD2 that copelleted with the histone H3/H4 beads was fractionated by 8% SDS–PAGE, and was detected by western blotting with the hFANCD2-specific mouse monoclonal antibody (FI17, Santa Cruz Biotechnology, Inc.).

For the recombinant hFANCD2-binding assay, the histone H3/H4 beads (15 µl) were incubated with purified hFANCD2, with or without 10 U of DNaseI (TOYOBO), at 23°C for 120 min. The beads were then washed three times with 100 µl of 10 mM PIPES-KOH buffer (pH 7.0), containing 0.5 M NaCl, 0.3 M sucrose, 1 mM $MgCl_2$, and 0.01% Triton X-100. The proteins bound to the beads were separated by 15% SDS–PAGE, and were visualized by Coomassie Brilliant Blue staining.

For the cFANCD2-binding assay, 293T cells were transiently transfected with GFP-cFANCD2-mutant plasmids, using Lipofectamine2000 (Invitrogen). Cells were disrupted in lysis buffer (Seki *et al*, 2007), and after the lysate was incubated with the histone H3/H4 beads (7.5 µl) at 4°C for 3 h, the beads were washed four times with lysis buffer. The proteins were separated by 6% SDS–PAGE, and were detected by western blotting with an anti-GFP Ab (Clontech).

Topological assay for nucleosome formation

Experimental procedures are described in Supplementary Materials and Methods.

Gel-shift assay for nucleosome formation

The H2A/H2B complex (8 ng/µl) and the H3/H4 complex (8 ng/µl) were pre-incubated with hFANCD2 or hNap1 at 23°C for 10 min. The nucleosome-assembly reaction was initiated by the addition of the 195 bp DNA (8 ng/µl) containing the *Lytechinus variegates* 5S ribosomal RNA gene (Osakabe *et al*, 2010) in a 10 µl reaction mixture, containing 20 mM Tris–HCl (pH 8.0), 140 mM NaCl, 7% glycerol, and 1 mM dithiothreitol. The reaction was continued at 23°C for 60 min, followed by a further incubation at 42°C for 60 min to eliminate the non-specific DNA binding by free histones. The samples were then separated by 6% PAGE in 0.2 × TBE buffer